Egypt. J. Bot. **Vol. 64**, No. 2, pp. - (2024)

Egyptian Journal of Botany
http://ejbo.journals.ekb.eg/

Green Synthesis and Characterization of Titanium Dioxide Nanoparticles by *Aspergillus niger* DS22 (ON076463.1) and Its Potential Application in Medical Fields

Dalia K. Abd El Hamid[(1)], Enayat M. Desouky[(1)], Sawsan AbdEllatif[(2)#], Nermine N. Abed[(1)], Amira Y. Mahfouz[(1)]

[(1)]Botany and Microbiology Dept., Faculty of Science (Girls), Al-Azhar University, Cairo, Egypt; [(2)]Bioprocess Development Dept., Genetic Engineering and Biotechnology Research Institute (GEBRI), City of Scientific Research and Technological Applications (SRTA-City), New Borg El-Arab, 21934, Alexandria, Egypt.

NANOMATERIALS have received much attention in the last two decades and have been introduced into most life fields, especially the medical field. Therefore, the present research aims to biosynthesize titanium dioxide nanoparticles (TiO_2NPs) by *Aspergillus niger* DS22 (ON076463.1) and evaluate its antibacterial, anti-inflammatory, and wound-healing activities. Forty-five fungal isolates were isolated from nine different Egyptian soil samples and tested for producing TiO_2 nanoparticles (NPs). The most potent fungal isolate that produced the promising potential TiO_2NPs was identified by 18S ribosomal RNA as *Aspergillus niger* DS22. The factors affecting the secretion of bioactive compounds assisted in TiO_2 nanoparticle biosynthesis were optimized. Gas chromatography-mass spectrometry (GC–MS) and High-performance liquid chromatography (HPLC) analysis of *Aspergillus niger* DS22 (ON076463.1) filtrate showed the existence of various active metabolites, which exhibited antibacterial and anti-inflammatory impacts. Results showed that TiO_2NPs were elliptical to spherical, ranging in size from 10.4 to 45.8nm with a size mean of 26.619±7.577nm. TiO_2NPs had antibacterial action versus five pathogenic bacterial strains. The maximum activity was against Methicillin-Resistant *Staphylococcus aureus* MRSA (ATCC 25923) (34mm inhibition zone) and the minimum activity was against *Klebsiella pneumonia* (ATCC 700603) (19.66mm inhibition zone). Also, TiO_2NPs exhibited inhibition percentages of human erythrocyte hemolysis (97.7%) at 1000µg/mL concentration compared with standard Indomethacin (98.6%). Besides, TiO_2NPs were effective in human dermal cells wound recovery after 48h by (65.96%) linked with control (58.49%). These findings evoked that TiO_2NPs have promising antibacterial, wound-healing, and anti-inflammatory actions, which may be an auspicious approach for pharmaceutical applications.

Keywords: Antibacterial, Anti-inflammatory activity, GC–MS, FTIR, TiO_2NPs, Wound-healing.

Introduction

One of the biosphere's most intricate, diverse, and significant assemblages of species is the soil microbial community. They are involved in a variety of biological processes, including the mineralization and decay of biotic materials, biocontrol, and antagonistic interactions (Hackl et al., 2004). Each microhabitat in an ecological niche is made up of a microscopic diversity including bacteria, fungi, actinomycetes, nematodes, and protozoa as well as a macroscopic diversity including insects, plants, and others (Striet & Schmitz, 2004). Nowadays, nanotechnology is indeed one of the new advancements that have made great progress over the past ten years and have attracted major scientific interest (Sharaf et al., 2022; Yahia et al., 2023). The most common category of microbes is the fungus, which has numerous

#Corresponding author email: sabdellatif@srtacity.sci.eg
Received 28/10/2023; Accepted 22/01/2024
DOI: 10.21608/ejbo.2024.245157.2550
Edited by: Prof. Dr. Neveen Mahmoud Khalil, Faculty of Science, Cairo University, Giza 12613, Egypt.

uses in the disciplines of enzyme production, bioremediation, and nanotechnology (Mohamed et al., 2019; Selim et al., 2021; Ahmed et al., 2022). Fungi received more consideration in studies on the biological production of metallic nanoparticles due to their tolerance and capacity for metal bioaccumulation. Additionally, they surpass bacteria in terms of producing nanoparticles in several ways (Salem, 2023). Production of fungal-based nanomaterials uses a bio-mineralization mechanism that involves biomolecules and external and internal enzymes reducing various ions of metal (Spagnoletti et al., 2019). More investigation into the production of nanomaterials has been carried out using the species of *Fusarium, Trichoderma, Aspergillus, Verticillium, Penicillium,* and *Rhizopus* (Salem & Fouda, 2021; Elsayed et al., 2022). Various shapes and sizes of TiO_2NPS can be obtained through fungal-mediated synthesis (Rajakumar et al., 2012; Durairaj et al., 2014; Hassan et al., 2020; Sagadevan et al., 2022). The sole naturally occurring form of titanium is titanium dioxide. TiO_2NPs have unique topologies and surface characteristics. The three different polymorphs of TiO_2NPs are anatase, rutile, and brookite. Rutile and anatase have tetragonal geometric symmetry and attributes including gloss, stiffness, and densities (Sagadevan et al., 2022). Estimates indicate that 4.68 million tons of TiO_2 were produced globally in 2009, and by 2014, the total amount produced had gone up by more than 9 million tons (Nasr et al., 2018; Kim et al., 2019; Ikram et al., 2021). TiO_2 is a high thermal stability, insoluble, fire-resistant, and non-hazardous metal oxide. TiO_2 has titanium with an atomic number of 22 from the IV B group and oxygen with an atomic number of 8 from the VI A group (Nabi et al., 2018; Ziental et al., 2020). Under normal circumstances, TiO_2 is a naturally hydrophobic powder that has no smell and is brightly white, has a broad band gap, and is a solid inert substance. It is a very stable compound that is also effective as an opacifier. TiO_2NPs are primarily used as a material for semiconductors due to their major characteristics including low price, strong oxidizing strength, elevated refractive index, elevated chemical stability, and the existence of functional groups containing oxygen in its lattice. TiO_2 is a nontoxic pigment, consequently, it can be used for producing ceramics, paints, plastics, paper, ink, rubber, textiles, cosmetics, and leather. Additionally, TiO_2 is frequently used as a pigment to add whiteness and opacity to commodities like sunscreen, coatings, medicines, food, and toothpaste (Verma et al., 2022). Besides that, the employing of titanium dioxide nanoparticles (TiO_2NPs) in the field of medicine, because of their excellent biocompatibility with body tissues, great medicinal potential, and inertia, biomedical applications such as prosthetic hips, bone plates, scaffolds, dental implants, coatings, and drug and gene delivery systems have been developed (Ikram et al., 2021). One of the major issues in clinical settings is the healing of infected wounds (Widyaningsih et al., 2023). Once a burning hurt or a surgical incision has occurred, bacteria quickly colonize the exposed wounds (Roy et al., 2020).The majority of the time, the microorganisms that colonize these wounds are either part of the patient's usual flora or have been transferred from polluted external sources such as water, food, or infected hands of medical personnel (Abbas et al., 2020). Several commonplace pathogens that can cause severe wound infections including *Staphylococcus aureus* and *Enterococcus* spp.(gram-positive bacteria) like *Acinetobacter* spp., *Pseudomonas aeruginosa* (gram-negative bacteria) and fungi like *Aspergillus* spp., and *Candida* spp. are all listed as typical pathogenic microbes that may result in trenchant infections of wounds, and many of them are antibiotic-resistant (Flowers & Grice, 2020). In many therapeutic situations, the dressings of the wound are put on a wound to stop infection spread and serve as a replacement for the skin covering temporarily (Sankar et al., 2014). Antibiotics have served as the first line of protection against a variety of deadly Gram-positive and negative microbial infections ever since the time of developing many antibiotics in the 21st century. The severe side effects of several antibiotics in humans because of the similarity between bacterial and human mitochondrial ribosomes (Javed et al., 2020). Antibiotic resistance is increasing, and the indiscriminate use of antibiotics has made it difficult to regulate human and animal restrictions (Ellatif et al., 2022). Because of this, it is necessary to develop efficient antimicrobial substances that are biocompatible, effective against microbial illnesses, and have minimal negative effects on human cells. This study concentrates on the fungal-mediated production of TiO_2NPs, which have overgrown potential in the biomedical area as antibacterial, wound-healing, and anti-inflammatory materials.

Materials and Methods

Chemicals and reagents

The chemicals and solvents were purchased from Sigma-Aldrich Chemical Co. (St. Louis Missouri, 63103, USA) and were of analytical purity. Water Agar medium, Richard's Agar medium, Czapek's Dox Agar medium, Martin's Rose Bengal Agar medium, Waksman's Agar medium, Sabouraud Dextrose Agar, Potato Dextrose Agar (PDA), Malt extract Agar, Nutrient Agar, Malt extract Yeast Extract Glucose Peptone (MYGP) broth medium and Potato Dextrose Broth (PDB) medium were obtained from Difco (United Kingdom).

Fungal isolation from different soil samples

Various soil samples were collected from different localities in Egypt (New Waddey Governorate – Damanhur city-El-Beheira Governorate – Benzene station in Damanhur, El-Beheira Governorate – Waddy Hof, Helwan Road - Red Sea Coast near Attaqa Mountain- Toshka, Aswan Governorate – New Borg El Arab City) and transposed in polythene sterilized bags to the laboratory. Serial dilutions for each soil sample were performed and used the suitable one. By plating the original inoculum on Czapek's Dox Agar medium (pH 7) with 0.1mL of soil sample suspension (10^{-5}) separately, the fungi were picked up. For 5-7 days, whole plates were incubated at 28 °C. After incubation, the plates were examined, and the fungal isolates were purified on the same medium as before. Purified isolates were sub-cultured on slants of the same media and stored at 4 ºC until further examinations.

Screening for metal tolerance ability of the fungal isolates

A maximum tolerance concentration (MTC) test was conducted to establish the ability of Ti^{+4} metal tolerance of the fungal isolates to potassium hexafluoro titanate (K_2TiF_6). The purified forty-five fungal isolates were grown at gradient higher concentrations of metal (50-350ppm). Isolated fungi exhibiting the greatest MTC value were chosen for further studies of nanoparticle production.

Biosynthesis of titanium dioxide nanoparticles by the selected fungal isolates

Each of the six fungal isolates showing the highest MTC value were inoculated in 100ml Malt extract Yeast Extract Glucose Peptone (MYGP) broth medium and incubated at 30°C in an orbital shaker at 200rpm for 72h. The fungal biomass afterward was obtained from the growing culture media by filtration within laminar flow by using sterilized Whatman filter paper, and the settled fungal biomass was gently washed triple with sterilized deionized water. The harvested biomass of six fungi (20g fresh weight) was then resuspended in sterilized deionized water (100mL) followed by incubation at the same condition before. After incubation, the fungal mycelia were harvested by using a centrifuge (5000rpm) for 20min at 10°C, and the filtrate was kept cold for TiO_2NPs biosynthesis. The filtrate devoid of fungal cells was mixed with Ti^{+4}salt solution (K_2TiF_6) (1mM) in volumes of 1:9 (v/v) and subsequently incubated at 30°C in 200rpm in an orbital shaker for 24h. in a dark condition. The bio-transformed product was gathered for characterization. The control was only fungal filtrate without metal ions (Raliya & Tarafdar, 2015).

Selection of the most potent fungal isolates for the smallest-sized nanoparticles biosynthesis of titanium dioxide

The bio-transformed product of each of the six fungal isolates was assessed by UV-visible spectroscopy in the range of 200-800nm. The highest value of absorbance in the spectra of UV–visible was selected and considered as the most potent fungal isolate, then the mixture of reaction was centrifuged for 30min at 10000rpm to precipitate the nanoparticles. The collected nanoparticles were re-dispersed in deionized water and centrifuged once more. The collected nanoparticles were washed accurately three times leastwise with deionized water to get rid of any of the biological contaminants present. After that, the nanoparticles were dehydrated in an oven at 50°C and used for size determination by scanning electron microscope (SEM) at Central Laboratories in Bioprocessing and Genetic Engineering Institute, City of Scientific Research and Biotechnological Applications, New Borg El-Arab City, Alexandria, Egypt. The most potent fungal isolate F_{25} was selected for further experiments throughout the current work.

Screening of the most potent fungal isolate extract fractions for the nanoparticle's biosynthesis of titanium dioxide

The most potent fungal isolate F_{25} extract was screened for the nanoparticle's biosynthesis

of titanium dioxide. The isolated fungus was grown on MYGP medium, pH 7.0±0.4, incubated in a 200-rpm shaking incubator at 30°C for two different incubation periods: three and seven days. After growing for 7 days, the fungal culture was filtered under an aseptic technique and the filtrate (extracellular fraction) was collected and used for the biosynthesis of titanium dioxide nanoparticles. After growing for 3 days, the fungal culture was filtered under an aseptic technique but in this case, the fungal biomass was collected and after washing triple to remove any medium component, used for biosynthesis of titanium dioxide nanoparticles in two different methods. Firstly, part of the fungal biomass (20g wet weight) was dispersed in sterilized Milli-Q deionized water (100mL) and subsequently incubated at 30°C in a 200-rpm shaking incubator for 72h. After that, filtration was carried out and the cell-free filtrate (periplasmic fraction) was collected and used for the biosynthesis of titanium dioxide nanoparticles. Secondly, the fungal pellets (20g fresh weight) were dispersed directly in (1mM) potassium hexafluoro titanate (K_2TiF_6) solution (100mL) and subsequently incubated at 30°C, dark and 200rpm shaking incubator for 24h. Afterward of incubation in the three cases, the synthesis of TiO_2NPs was checked for color changing to white. By then UV-visible spectrophotometer analysis of the reaction mixture was further used to confirm the biotransformation. The spectrum was scanned in the range of 200–800nm using a UV-vis spectrophotometer (Model: 20 Spectronic, Arthur H. Thomas Co. USA). The control was only fungal filtrate without metal ions (Raliya & Tarafdar, 2015).

The most potent TiO_2NPs producer fungal isolate (F_{25}) identification

Morphological identification

The most potent fungal isolate F_{25} was subjected to examination by a light microscope with 10 and 40X lens power to determine the shape of mycelium and conidia. F_{25} was allowed to grow in eight different cultivation media Potato Dextrose Agar (PDA), Malt extract agar, Water Agar, Richard's Agar, Czapek's Dox Agar, Martin's Rose Bengal Agar, Waksman's Agar, and Sabouraud Dextrose Agar. Three replications were maintained for each media.

Molecular identification

The confirmatory molecular identification of fungal isolate (F_{25}) was carried out based on a sequence of conserved ribosomal internal transcribed spacer (ITS) region using ITS1,4 primers using universal primer pairs ITS1 (50-TCCGTAGGTGAACCTGCGG-30) and ITS4 (50-TCCTCCGCTTATTGATATGC-30) (White et al., 1990). Amplification of ITS region was performed on a Thermal Cycler (Applied Biosystems 9700) with 25µL reaction mixtures containing 2.5mM MgCl2; 2.5µL of 10X buffer; 25 pmol ml_1 primer; 2mM each of dNTP; 1U of Taq DNA Polymerase; 50ng genomic DNA. The amplification cycle consists of an initial denaturation at 95°C for 50sec. followed by 30 cycles at 95 °C for 40 s, 50°C for 1min, 72°C for 1min, and a final extension at 72°C for 10min. Genetic identification of the fungal isolates was performed according to Elsehemy et al. (2020). Following the manufacturer's instructions, The DNA of the fungal isolate genome was extracted using the Biospin Fungus Genomic DNA Extraction Kit (Bioer Technology Co., Ltd., Hangzhou, P. R. China). The nucleotide sequences of the fungal isolate were submitted to GenBank for accession number. Next, the consensus sequences of a fungal isolate were subjected to a BLAST search to assign putative similarities http://blast.ncbi.nlm.nih.gov/Blast.cgi is an NCBI database. The operational taxonomic unit (OTU) for the fungal isolate was subsequently created using measures of sequence similarity and inferences from phylogenetic trees. Clustal X, (MEGA) software version, and BioEdit were used to compare the sequences to other comparable sequences that had been downloaded from GenBank.

Optimization of culture conditions for maximizing of total protein secretion for titanium dioxide nanoparticles (TiO_2NPs) biosynthesis by the most potent fungal isolate F_{25}

Different factors were investigated to optimize the biosynthesis of titanium dioxide nanoparticles by optimizing fungal cell-free filtrate production of F_{25} viz. different culture media (MGYP media (g/L) (Malt extract, 3.0; Glucose, 10.0; Yeast extract, 3.0 and Peptone, 5.0, PDB media, modified MGYP media(g/L)(Glucose, 15.0; Yeast extract, 3.5 and Peptone, 10.0 and KNO_3, 3.5) (Tarafdar et al., 2013) and basal media containing (g/L) KH_2PO_4, 7.0; K_2HPO_4, 2.0; $MgSO_4 \cdot 7H_2O$, 0.1; $(NH_4)_2SO_4$, 1.0; yeast extract, 0.6; and glucose, 10.0 (Zomorodian et al., 2016), pH values (4 to 9), incubation temperature (10, 20, 25, 30, 35, and 45ºC), shaking and static

conditions, incubation period (from one day up to six days). Different concentrations of modified MGYP media constituents were applied in separate times, i.e. different peptone concentrations (0.5, 1, 1.5, 2, 2.5 and 3%) (w/v), Different yeast extract concentration (0.15%, 0.25%, 0.35%, 0.45%, 0.55%, and 0.65%) (w/v), Different KNO_3 concentrations (0.15%, 0.25%, 0.35%, 0.45%,0.55%, and 0.65%)) (w/v) and Different glucose concentrations (0.5, 1, 1.5, 2, 2.5 and 3%) (w/v). The broth medium in each case was prepared and distributed into 250mL conical flasks, 100 ml for each flask. Flasks were inoculated and incubated in a shaking incubator at 200rpm for 4 days. The experiments were conducted as previously mentioned in TiO_2NPs biosynthesis until the fungal biomass-free filtrate was obtained. The various factors and effects were evaluated by estimation of the total content of protein in the fungal biomass free filtrate according to Lowry (1951). The estimations were carried out in triplicate and the results were recorded as (mean± SD).

Screening of bioactive compounds secreted by F_{25} fungal isolate in addition to studying the role of enzyme

Identification and studying the role of bioactive compounds produced by fungal isolate F_{25} which participate in the biological synthesis of titanium dioxide nanoparticles was done by different techniques and tests to illustrate their role in this bioprocess.

A- Gas Chromatography/Mass Spectroscopy analysis of the cell-free filtrate of the most potent fungal isolate F_{25}

Gas chromatography in combination with mass spectrometry (GC/MS) was applied to determine the chemical components by using a Shimadzu GC–MS-QP 2010Plus outfitted with an RTX-5 (60mml, 9 0.25 mml, D., 90.25µm) capillary column in JNU, New Delhi, with helium as a carrier at 300°C, according to the methodology provided by Soliman et al. (2022).

B- High-performance liquid chromatography analysis of cell-free filtrate of the most potent fungal isolate F_{25}

The phenolic and flavonoid compounds in F_{25} biomass-free filtrate were evaluated using the methodology outlined by Gini & Jeya Jothi (2018). Ten mL of the filtrate was injected into a High-performance liquid chromatography (HPLC) system from the Agilent 1100 Infinity series fitted with an SPD-M10Avp diode array detector for quantitative analysis. The polyphenols of F_{25} cell-free filtrate at 280nm, were detected. On the HPLC chart, the resolution peaks have been described in depth concerning the times of retention of each component. The resultant data were presented as micrograms per gram of dry sample weight (g/mL).

C- Estimation of total protein secretion and activity of reductase enzyme produced in the fungal cell-free filtrate by fungal isolate $F_{25.}$

Total protein content was estimated as previously mentioned. Also, reductase activity was detected and investigated over 5 days using the assay of nitrate reductase in the fungal-free filtrate following the process outlined by Hamedi et al. (2013) and Ottoni et al. (2017). By using UV-visible spectrophotometry at 540 nm, the absorbance of the resulting pink solutions was assessed. Based on the rise in the solution's nitrite concentration, the fungus cell-free filtrate's activity of enzyme (reductase) was identified.

D- Reductase enzyme purification by applying column chromatography and further purification by Sodium dodecyl sulfate-polyacrylamide gel electrophoresis (SDS-PAGE)

The fungal biomass-free filtrate was further partially purified by Ammonium Sulphate precipitation (Atta et al., 2009; Soliman et al., 2023). Dialysis was carried out in a special pre-treated plastic bag against 50 mM sodium phosphate buffer (pH 7.0) overnight. The dialysis buffer was changed 3–4 times over a 24 hr. period (Muhammad et al., 2015). The dialysate partially purified preparation was applied to a column packed with Sephadex G-75, as mentioned by Naz et al. (2015), and Soliman et al. (2023). Preparation of the gel column and the fractionation procedure were carried out, and the harvested fractions were tested for reductase activity.

The purity of the most active fraction was checked by SDS-PAGE, which is used, also, for estimation of the molecular weight of the bioactive protein compared with a marker protein according to Laemmli (1970). These steps were considered complete purification for reductase enzyme since it had a great role in titanium dioxide nanoparticles biosynthesis.

Characterization of TiO_2NPs synthesized by F_{25}

fungal isolate under optimized conditions

1. Particle Size Analyzer (PSA)

Titanium dioxide nanoparticles powder sample was analyzed for their particle-size distribution with a particle-size analyzer (Mastersizer SVer. 2.19, Malvern Instruments Ltd, Worcestershire, UK) at Central Lab of Advanced Technology and New Materials Research Institute, City of Scientific Research and Biotechnological applications, New Borg El-Arab City, Alexandria, Egypt.

2. Transmission Electron Microscope (TEM)

Transmission electron microscopy (TEM) measurements were made utilizing the drop coating method to verify the size and shape (Subbaiya, 2017) using JEOL GEM-1010 Transmission Electron Microscope at 80kV (Amin et al., 2021).

3. Energy Dispersive X-ray (EDX)

Thermo-Noran EDX attachment was used for elemental analysis (Scimeca et al., 2018).

4. Fourier Transformation Infrared spectroscopy (FTIR)

Using a SHIMADZU FT-IR (Germany) spectrophotometer model, infrared spectra of solid samples were captured spanning a spectral area from 4 000 to 650 cm-1. Using the Perkin Elmer Spectrum GX FT-IR and the Spectrum v 5.3.1 software, spectra for samples in solution form were collected over a spectral area from 10,000 to 300,000 cm-1. Quartz cuvettes were used to analyze liquid samples.

5. X-ray diffraction (XRD) analysis

Measurements of X-ray diffraction of both the commercial TiO_2 and biologically synthesized titanium dioxide NPs were recorded on an X–ray diffractometer (Philips Analytical). The particle size, phase variety, and identification material of the TiO_2NPs were recognized. The samples were collected in lids and put under the device for analysis (Hassan et al., 2020).

Biomedical application of Titanium dioxide nanoparticles biosynthesized by the fungal isolate F_{25}

Antibacterial activity

The antibacterial activity of the bio-synthesized titanium dioxide nanoparticles was examined against various clinical pathogens using a well diffusion technique according to the method explained by Soliman et al. (2023). Nutrient agar plates were prepared and swabbed with different strains of pathogenic bacteria and wells were prepared on the agar followed by the addition of 100µL of fungal-free filtrate, K_2TiF_6 solution, biosynthesized TiO_2NPs (75µg /0.1mL), antibacterial standard (Amoxycillin 85µg /0.1mL) The plates were incubated overnight at 37°C. After the incubation period, the mean of the inhibition zone diameters was measured in mm.

Evaluation of wound-healing activities of biosynthesized TiO_2NPs by scratch assay test

The effect of TiO_2NPs on the experimental healing of wounds was studied via the methodology of scratch assay. Dermal cell lines' adherent cell surfaces were scratched with a pipette tip to produce an artificial damaged region in the cell line. Following that, photographs of cell migration during the wound-healing process were taken (Fushimi et al., 2012). Herein, these cell lines were acquired from the Egypt's Cancer Institute in Cairo, Egypt. As reported by Cormier et al. (2015), cell cultivation was carried out in six multi-well plates until confluent. To keep the scratch size to the lowest value, a linear scratch was made using a yellow micropipette tip that had been sanitized and oriented at a 30-degree angle. The scratch was then exposed to treatment with titanium dioxide nanoparticles for 48 hr. The imaging of mutually wounded edges was then beheld using a 10X objective lens.

Anti-inflammatory activities

The potential of Titanium dioxide nanoparticles to reduce inflammation was examined utilizing the human red blood cell membrane stabilization technique according to Shinde et al. (1989), Anosike et al. (2012), and Elbestawy et al. (2023). By measuring the amount of supernatant hemoglobin, the inhibition of HRBC hemolysis was established. The hemoglobin content absorbance (OD) was determined at 540 nm wavelength using a spectronic (Milton Roy) spectrophotometer. By assuming that all hemolysis produced in the presence of distilled water is 100%, the percentage of hemolysis was estimated. The samples' percentage inhibition of hemolysis was calculated:

$$\% \text{ Inhibition of haemolysis} = 1-((OD_2-OD_1)/(OD_3-OD_1)) * 100$$

where: OD_1 is the test sample's absorbance in

an isotonic solution, OD_2 is the test sample's absorbance in a hypotonic solution, and OD_3 is the control sample's absorbance in a hypotonic solution.

Statistical analysis

Most Data in this investigation were presented as the mean ± standard deviation (SD). Statistical analysis was performed by one-way ANOVA test using the SPSS version 19 software package (SPSS, Chicago, IL, USA). A P value < 0.05 was considered significant.

Results and Discussions

In this study, forty-five fungal isolates have been isolated from nine soil samples. Screening for their metal tolerance ability against metal (Ti^{+4}) was also studied. All fungal isolates could grow at gradient-elevated concentrations of such metal. The metallotolerance ability of different fungal isolates represented in (Supplementary materials Fig. S1) indicates that only six fungal isolates exhibited the highest growth ability on higher metal concentrations (up to 350ppm), so they were potential isolates and were selected for further nanoparticles production studies. The (Supplementary materials Fig. S2) shows the pure culture of different six fungal isolates having the potential to tolerate increased concentrations of titanium salt precursor. Another investigator, (Raliya et al., 2013) illustrated that only 14 fungal isolates out of more than one hundred were found to be proficient in breaking down macro-scale precursor salt particles (TiO_2). Additionally, Tarafdar et al. (2013) revealed that twenty-five fungal strains were isolated from Indian soil and screened for titanium tolerance ability, only *Aspergillus tubingensis* TFR5 can grow at high concentrations of TiO_2 0.1M, so it has been used in further studies for TiO_2 nanoparticles production. Also, AbdElmohsen (2020) explained that twenty fungal isolates isolated from eight different samples of drinking water showed metallotolerance ability against gradient concentrations of Ti^{+4} metal.

Selection of the most potent fungal isolates for the biogenic synthesis of the smallest TiO_2NPs

The six fungal isolates (F_{25}, F_{27}, $F_{33,}$ F_{34}, $F_{37,}$ and F_{44}) produce an obvious color variation of the filtrate, and the highest peak at a wavelength of 350nm, but the titanium dioxide nanoparticles (TiO_2NPs) spectra that showed from each of these fungal isolates was of different values. At this wavelength, the supreme absorption intensity correlated to TiO_2NPs produced by F_{25} with an optical density of 1.142 OD, and the intensity of absorption decreased in $F_{37,}$ $F_{33,}$ $F_{44,}$ $F_{34,}$ and F_{27}, with optical densities of 0.740 0.500, 0.362, 0.248 and 0.232 OD respectively (Supplementary Materials Fig. S3).

Additionally, the particle size analysis of TiO_2NPs biosynthesized by the different six fungal isolates was determined using a Scanning Electron Microscope (SEM), and the data were listed in (Table 1). The results revealed that the average size of TiO_2 NPs for the six fungal isolates varied. F_{25} fungal isolate produced the smallest size of TiO_2NPs, an average size of 55-77 nm and a mean particle size of 65nm whereas F_{44} produced the largest TiO_2NPs with an average size of 110-240nm and a mean particle size of 190nm. Al-Garni et al. (2009) announced that a range of fungus isolates responded differently to varying metal concentrations. There were physiological and morphological variances amongst fungal taxa, species, and strains, consequently their responses to metal ion concentrations differed.

TABLE 1. Particle size analysis of TiO_2 nanoparticles biosynthesized by the different six fungal isolates

Fungal isolates	Size range (nm)	Particle size (nm) (mean ± SD)
F_{25}	55-77	65±7.164728
F_{27}	9-152	104±49.0815
F_{33}	88-121	90.5±14.3489
F_{34}	96-190	138.5±29.5087
F_{37}	50-110	90±18.0907
F_{44}	110-240	190±77.0783

Identification of the most potent fungal isolate (F_{25}) for Titanium dioxide nanoparticles production

A- *Morphological characterization of the most potent fungal isolate F_{25}*

According to methodologies stated by McClenny (2005) for the identification of *Aspergillus* species, the macroscopic and microscopic investigations illustrated that the TiO_2NPs producer isolate was identified as *Aspergillus niger* DS22. The colony showed overhasty growth with fluffy, woolly black mycelium on PDA. The best growth was recorded on Waksman agar medium and malt extract agar media followed by Czapek's Dox agar medium and Rose Bengal agar medium. The lowest mycelial growth was recorded on the Sabouraud dextrose agar and Richard's agar medium, while the Water agar medium did not support the mycelial growth of fungal isolate $F_{25.}$ The isolate exhibited no variations concerning colony color on different media as shown in the (Supplementary materials Fig. S4). The results of the examination by light microscope with 10 and 40X lenses power revealed that the mycelium is non-septate with globose conidia (Supplementary materials Fig. S5).

B- *Molecular Identification*

Using BLAST and FASTA inquiries, as well as directly comparing with possibly linked taxa, the genetic sequence of the 18S rRNA gene of the nuclear-encoded rRNA (566bp) of the promising *Aspergillus niger* DS22 was studied. The sequence examination revealed significant alignments 97-100% with high homology with chosen *Aspergillus niger* strains using Clustal X and was assigned and deposited in GenBank under the accession number (ON076463.1). Following the initial inspection of the *Aspergillus niger*18S rRNA gene sequence and sequences of the comparable strains retrieved from the Gene Bank dataset, the creation of a phylogenetic tree was conducted using MEGA 6.0 software, as shown in Fig. 1**.**

Screening of the most potent fungal isolate extract fractions for the biosynthesis of TiO_2NPs

The formation of TiO_2NPs (Supplementary materials Figure S6) was observed by color changing to white, which was verified by UV-vis spectroscopy of the reaction mixture at 350nm. The UV–visible spectra of colloidal TiO_2NPs biosynthesized at different localities of the fungal isolate *Aspergillus niger* DS22 (ON076463.1) was shown in Fig. 2. As compared to conventional techniques, fungal culture can be easily managed during nanoparticle production. The use of extracellular-produced enzymes, in particular, has the benefit of getting vast quantities in a reasonably pure state (Raliya et al., 2013). Also, the biosynthesis of TiO_2NPs by the mycelium-free filtrate of *Aspergillus* was informed by Raliya et al. (2013) and Raliya & Tarafdar (2015). Moreover, AbdElmohsen (2020) used the fungal biomass of *Aspergillus tubingensis* in the synthesis of titanium dioxide nanoparticles.

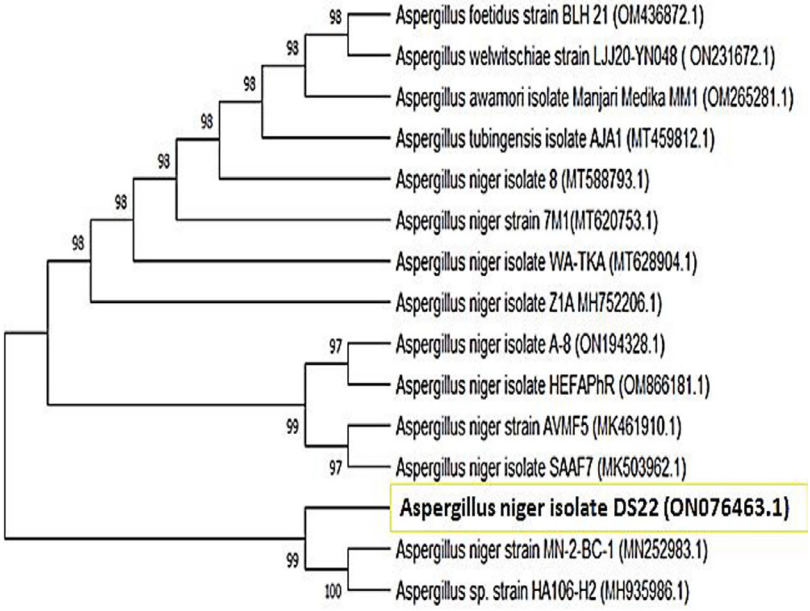

Fig. 1. A dendrogram showing the sequence relationships between *Aspergillus niger* DS22 (ON076463.1) (the most potent TiO_2 nanoparticles producer) and other *Aspergillus niger* strains using the sequencing ITS DNA region

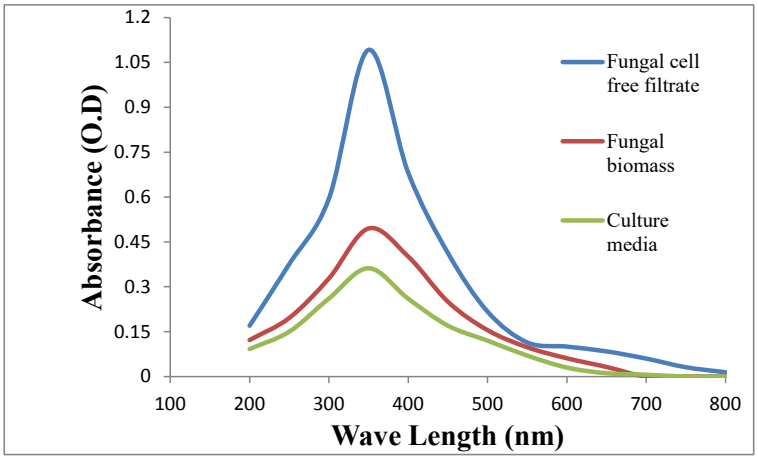

Fig. 2. UV–visible spectra of colloidal TiO_2NPs biosynthesized at different localities of the fungal isolate *Aspergillus niger* DS22 (ON076463.1)

Optimization of culture conditions for maximizing total protein secretion for titanium dioxide nanoparticles (TiO_2NPs) biosynthesis by Aspergillus niger DS22 (ON076463.1)

Previous studies showed the secretion of some proteins into the medium by the fungi might play an important role in the biotransformation and reduction of titanium ions into the TiO_2 nanoparticles, also capping protein which encapsulates the formed nanoparticles increasing the stabilization of TiO_2 NPs (Raliya et al., 2015; Rathore et al., 2023). Herin, the results recorded in (Supplementary Materials Table S1) concluded different culture conditions affecting total protein (mg/mL) secreted by *Aspergillus niger* DS22 (ON076463.1). Data showed that the modified MYGP medium was the most favorable medium as it showed the highest protein content. Maximum protein content in the fungal cell-free filtrate of *Aspergillus niger* DS22 (ON076463.1) was also achieved when the pH value of the medium was adjusted at 6 and the incubation process was carried out for 4 days at 30°C and 200rpm. In addition to these different parameters, media components played a vital role in the protein secretion in the fungal cell-free filtrate. Data revealed that maximum values of the protein content were noticed when Peptone conc. was (0.5%, w/v), Yeast extract conc. (0.15%, w/v), KNO_3 conc. (0.25%,w/v) and Glucose conc. (2%, w/v).

Screening of bioactive compounds secreted by Aspergillus niger DS22 (ON076463.1) in addition to studying the role of enzyme

To investigate the bioactive compounds, present in the fungal cell-free filtrate of *Aspergillus niger* DS22 and played a role in the biosynthesis of TiO_2NPs, many procedures were applied to achieve this investigation as follows:

Gas Chromatography/Mass Spectroscopy (GC/MS) analysis for the fungal cell-free filtrate of Aspergillus niger DS22 (ON076463.1)

In this study, the bioactive substances in the lyophilized cell-free filtrate of *Aspergillus niger* DS22 (ON076463.1) were detected by GC-MS analysis (Fig. 3). The chemical compounds' names, classes, as well as associated peaks at different retention periods and the molecular formula of analyzed *Aspergillus niger* DS22 (ON076463.1) cell-free filtrate were represented in (Table 2). GC-MS analysis showed the occurrence of 20 compounds. Three peaks appeared as the biggest peaks, peak 18 was the highest which had a peak area of 25.147% and had been recorded at a retention time of 45.638min. Also, peaks 6 and 17 showed height but less than peak 18 with peak areas of 10.447 and 10.019% at retention times of 10.514 and 45.532min respectively in addition to several minor peaks representing other compounds in little amounts. These peaks (which consisted of compounds like 1,2,3,4,6-Penta-trimethylsilyl Glucopyranose, Trimethylsilyl ether-glucitol and Octadecanamide, N- (2- methyl propyl)-N-nitroso) could be attributable to amino acid residues in protein molecules, since these compounds are linear nitrogenous compounds have long carbon chains (C16-C18) which can contribute with better interaction and can be protonated in the presence of other compounds (Rocha et al., 2020), indicating the production of certain proteinic substances into cell-free filtrate of *Aspergillus niger* DS22 (ON076463.1). On the other side, as a result of its anti-angiogenesis implications and controlling

functions of signal pathways such as autophagy, apoptosis, and the arrest of the cell cycle of cancer cells, oridonin is frequently utilized for relieving pain and inflammation associated with cancer such as carcinoma of the liver, cancer of the breast, carcinoma of the gall bladder, cervical carcinoma, and carcinoma of the mouth and to manage such cancer diseases (Abdullah et al., 2021; El-Baba et al., 2021), and has antioxidant effects (Wu & Zhou, 2023). Similar to previous research, the compounds or their derivatives realized in this research, such as Octadecanamide, N- (2- methyl propyl)-N-nitroso,1-Dodecene, Tetradecane, and Cyclodecane, have antibacterial, antioxidant, antitumor, and anti-inflammatory properties (Mokhtar et al., 2023).

HPLC analysis for the fungal cell-free filtrate of Aspergillus niger DS22 (ON076463.1)

The results of the HPLC chromatogram of the lyophilized fungal cell-free filtrate of *Aspergillus niger* DS22 (ON076463.1) showed the presence of different phenolic and flavonoid compounds which were recorded at varying times of retention, concentrations, and biological activities as shown in Table 3 and Fig. 4. 4, 3 indul butyl acetic acid was detected in high quantity (10.171g/mL), subsequently followed by Gallic acid (9.453g/ml), and Coumarine (8.891g/mL), while Cinnamic acid was reported in a small amount (1.363g/mL), also the existence of Vanillic acid, Naphthyle acetic acid, and Pyrochatechole but in moderate concentrations (6.241µg/ml,5.701µg/mL, and 3.081µg/mL, respectively). The metabolic profile indicates the presence of several compounds of pharmacological and biological importance. Compared with other fungi, *Aspergillus* species is one of the most prevalent fungi and can generate the most physiologically active secondary metabolites (Mokhtar et al., 2023). Several bioactive compounds produced by *Aspergillus* species were classified as terpenoids, alkaloids, steroids, lignans, quinones, acetones, and phenols (Abdel-Wahhab et al., 2020). Many biological activities were documented in other investigations utilizing these flavonoid and phenolic compounds. For instance, antiangiogenic, antioxidant, and antitumorigenic effectiveness were attributed to cinnamic acid (Niero et al., 2013; Mashraqi et al., 2023). Gallic acid has been investigated to have anti-HCV activity, and immunomodulatory effects (Bai et al., 2021; Mashraqi et al., 2023). Moreover, Ellatif et al. (2022) illustrated that 4, 3 indul butyl acetic acid displayed several therapeutic activities such as antidiabetic, anticancer, antibacterial, anti-HIV, antiviral, anti-inflammatory, and antioxidant activities**.** Other flavonoid and phenolic compounds with their biological activities were summarized in Table 4.

Estimation of total protein secretion and reductase activity produced by Aspergillus niger DS22 (ON076463.1)

To investigate the role of other bioactive compounds in the extracellular biosynthesis of TiO_2 nanoparticles, total protein secretion, and NADH-dependent reductase were estimated. Total protein content was recorded in the fungal cell-free filtrate (1.2628mg/mL).

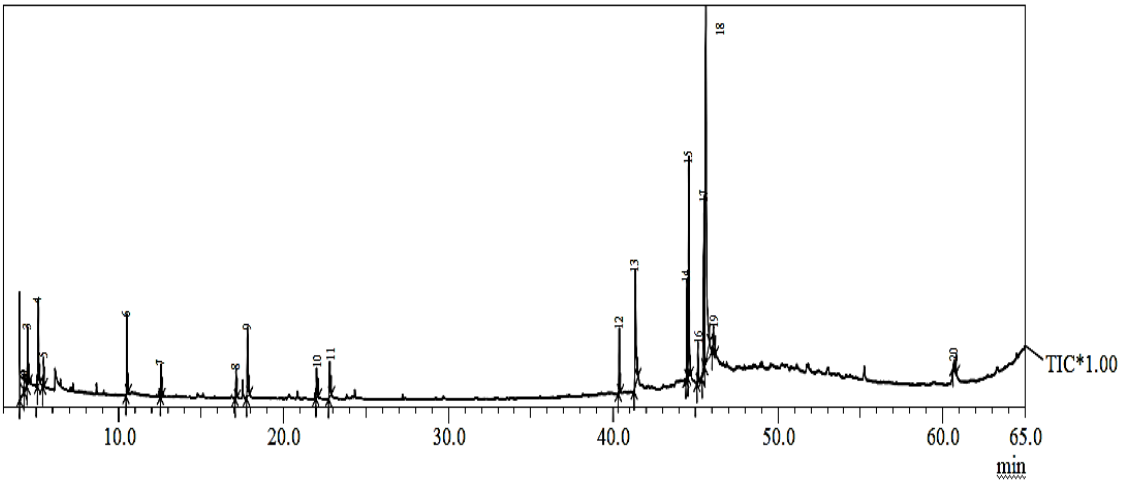

Fig. 3. GC-mass spectral analysis of lyophilized fungal cell-free filtrate of *Aspergillus niger* DS22 (ON076463.1)

TABLE 2. Quantitative results of GC-mass spectral analysis of lyophilized fungal cell-free filtrate produced by *Aspergillus niger* DS22 (ON076463.1)

ID	R. time (min)	Peak area (%)	Compound name	Retention index (RI)	Molecular formula
1	2.945	0.0509	6-Acetyl-ß-d-mannose	785	$C_6H_{14}O_7$
2	4.324	0.4034	2-Furancarboxaldehyde,5-methyl	688	$C_6H_6O_2$
3	4.493	5.0742	1-Dodecene	718	$C_{10}H_{21}CH{=}CH_2$
4	5.134	4.5635	Tetradecane	975	$C_{14}H_3O$
5	5.451	3.0223	Cyclodecane	887	$(CH_2)_{12}$
6	10.514	10.4478	Oridonin	861	$C_{20}H_{28}O_6$
7	12.586	1.5249	2,4-Ditert-butylphenol	793	$C_{14}H_{22}O$
8	17.140	1.1495	24,25-Dihydroxycholecalciferol	967	$C_{27}H_{44}O_3$
9	17.837	3.6239	Butylated hydroxytoluene	957	$C_{15}H_{24}O$
10	22.029	3.0622	2,4-Ditert-butylphenol	826	$C_{14}H_{22}O$
11	22.816	6.2866	Dibutyl phthalate	746	$C_{16}H_{22}O_4$
12	40.381	4.3769	N-didehydrohexacarboxyl-2,4,5-trimethylpiperazine	945	$C_{13}H_{22}N_2O$
13	41.371	5.5684	alpha-D-Glucopyranoside, methyl 2,3,4,6-tetrakis-O- (trimethylsilyl)-	1173	$C_{19}H_{46}O_6Si_4$
14	44.492	3.2040	Heptasiloxane, Hexadecamethyl-	1021	$C_{16}H_{48}O_6Si_7$
15	44.609	6.2479	Octadecanamide, N- (2- methyl propyl)-N-nitroso	946	$C_{22}H_{44}N_2O$
16	45.153	2.5756	5Z,8Z,11Z-eicosatrienoic acid	694	$C_{20}H_{32}O_3$
17	45.532	10.0192	Trimethylsilyl ether-glucitol	749	$C_{24}H_{62}O_6Si_6$
18	45.638	25.1478	1,2,3,4,6-Penta-trimethylsilyl Glucopyranose	792	$C_{21}H_{52}O_6Si_5$
19	46.080	1.7403	Didodecyl 3,30 –Thiodipropionate	1028	$C_{30}H_{58}O_4S$
20	60.715	1.9105	Bis (2-ethylhexyl) phthalate	973	$C_{30}H_{58}O_4S$

TABLE 3. Tentative results of High-performance liquid chromatography analysis of lyophilized fungal cell-free filtrate produced by *Aspergillus niger* DS22 (ON076463.1)

Retention time (min)	Constituent name	Area	Area (%)	Concentration (µg/mL)	Biological activity
2.874	Gallic acid	156.439	6.042	9.453	Anti-HCV activity, immunomodulatory effect (Bai et al., 2021; Mashraqi et al., 2023)
5.923	Vanillic acid	18.704	3.336	6.241	Antioxidant, anti-inflammatory, and neuroprotective properties, an anti-filarial, antimicrobial impact (Salau et al., 2020; Ullah et al., 2020; Ellatif et al., 2022)
6.183	Pyrochatechole	36.406	8.462	3.081	Antioxidant and anti-inflammatory effects, anti-HBV activity (Ellatif et al., 2022)
11.891	Coumarine	34.055	2.611	8.891	Antiviral activity
13.153	Cinnamic acid	7.837	1.738	1.363	Antiangiogenic, antioxidant, and antitumorigenic effectiveness (Niero et al., 2013; Mashraqi et al., 2023).
14.845	4,3 indul butyl acetic acid	75.926	1.339	10.172	Antidiabetic, anticancer, antibacterial, anti-HIV, antiviral, anti-inflammatory, and antioxidant (Ellatif et al., 2022).
17.340	Naphthyle acetic acid	7.241	7.873	5.701	Antibacterial and antifungal activity (Gowri et al., 2013)

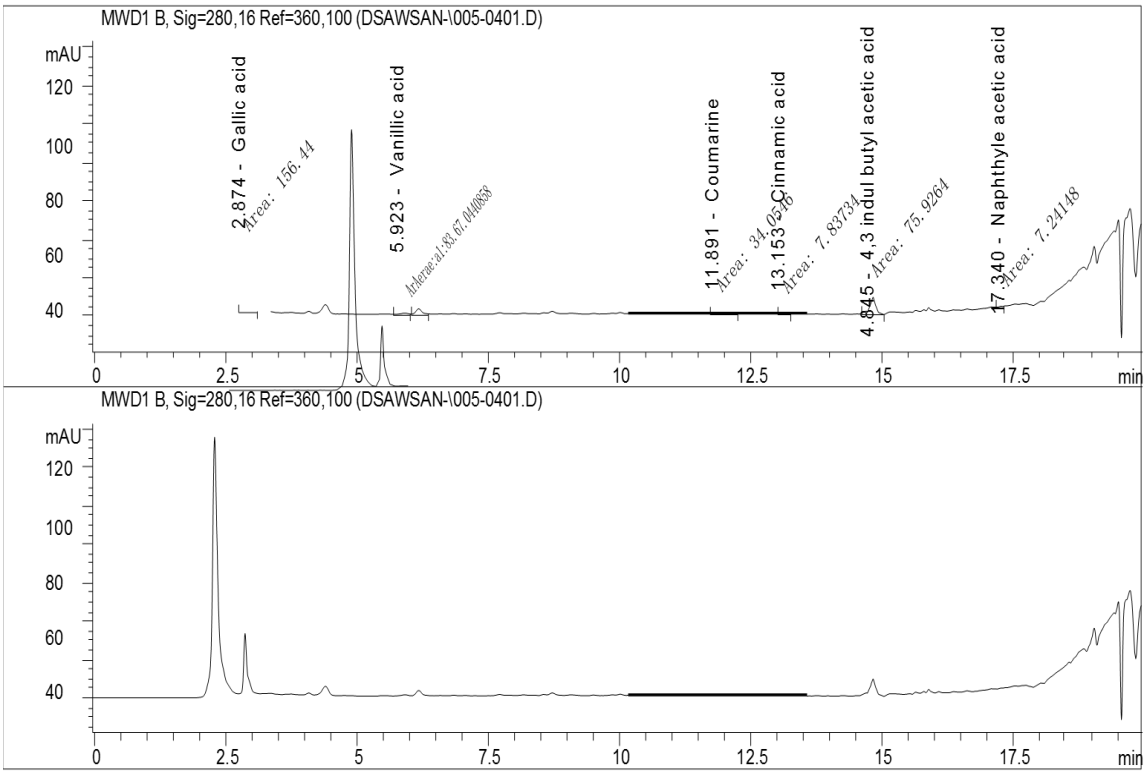

Fig. 4. High-performance liquid chromatography of detected flavonoid and phenolic compounds in lyophilized fungal cell-free filtrate produced by *Aspergillus niger* DS22

The enzymatic activity of the fungal cell-free filtrate was assessed based on the increase in nitrite concentration of the filtrate and presented as nmol nitrite/mL.day. This enzyme was secreted by *Aspergillus niger* DS22 (ON076463.1) and may be accountable for Ti^{+4} ions reduction and the formation of TiO_2NPs. As shown in (Fig. 5 and Supplementary Materials Table S2), there was a rational association between reductase activity and the efficacy of *Aspergillus niger* DS22 (ON076463.1) in the biosynthesis of TiO_2NPs. Overall, the enzyme converts nitrate to nitrite and then stimulates the electron shuttle to reduce the dispersed metal ions to their nanoform parallels, resulting in a continual series of oxidation-reduction reactions (Mukherjee et al., 2018; Eltarahony et al., 2021). Despite this, nitrate reductase enzymes, which are essential in regulating AgNP production, have been identified at the molecular and chemical levels. Additionally, numerous studies have postulated that NADH-dependent NO_3- reductase (NR) participates with a powerful role in the synthesis of NPs (Au, Fe, Cu, Ti etc.) as a catalytic biomolecule (Avilala & Golla, 2019).

Reductase enzyme purification by applying column chromatography and further purification by Sodium dodecyl sulfate-polyacrylamide gel electrophoresis (SDS-PAGE)

Data represented graphically in (Supplementary Materials Figure S7 and Supplementary Materials Table S3) showed that fraction number 1 had the maximum total protein concentration (1.3221mg/mL) and the maximum nitrate reductase activity (60.9412nM nitrite/ml h) and hence it had the highest activity in biosynthesis of TiO_2NPs. The purity of fraction NO. 1 was confirmed by SDS-PAGE. The molecular weight of the pure protein (reductase enzyme) was estimated at 140kDa. The (Supplementary Materials Fig. S8) indicated that the purified protein compound produced by *Aspergillus niger* DS22 (ON076463.1) contained a single protein band. Extracellular microbial enzymes are important reducing agents in the creation of metallic nanoparticles (Subbaiya et al., 2017). According to research, cofactors like nicotinamide adenine dinucleotide (NADH) and reduced form of nicotinamide adenine dinucleotide phosphate (NADPH) dependent enzymes both play important roles as reducing

substances through the transport of electrons from NADH via NADH-reliant enzymes that serve as electron carriers (Bose & Chatterjee, 2016). When the author utilized baker's yeast (S. cerevisiae), the creation of titanium dioxide nanoparticles could have been caused by a pH-sensitive membrane-bound oxidoreductase enzyme, according to Jha et al. (2009).

Characterization of TiO_2NPs biosynthesized by Aspergillus niger DS22 (ON076463.1)

The visual observation of the cultures verified the production of TiO_2NPs, as the color of the growth media altered from colorless transparent to a blurred pale white color through the process, and finally distinguished coalescent white deposits were noticed at the bottom of the cultivated bottle, indicating the synthesis of TiO_2NPs. The average particle size of TiO_2NPs was 26.25nm as shown in Fig. 6. On the other hand, TEM results demonstrated that the shape of the particles was spherical and ranged from spherical to elliptical, the particle's size concerning the spherical shape ranged from 10.4 to 45.8 nm with a size mean of 26.619±7.577 nm and the nanoparticles were existing in a monodisperse stage which showing a certain degree of agglomeration (Fig. 7).

The elemental report of the bio-prepared TiO_2 NPs approved that Ti^{+4} and O^{-2} atoms are the main constituent elements, which confirms the purity of TiO_2NPs composition. As shown in Fig. 8, strong unique elemental peaks were recorded at 3.5 and 4.5ke V with weight percentages around 65 and 35% respectively. Based on the outcomes of other researchers, these results agreed with Tarafdar et al. (2013) who recorded that, the size of the TiO_2 nanoparticle formed by fungal-free filtrate *Aspergillus* spp. was calculated using dynamic light scattering (DLS) ranged from 1.5 to 30nm. TEM was used and results displayed that the particles were in the nano range and monodispersed. The purity of the TiO_2NPs formulation was validated using the EDX technique. Also, Raliya & Tarafdar (2014) reported that the size distribution of TiO_2NPs formed by A. terreus is lower than 6nm with a surface charge of – 6.25mv as measured by DLS. Results from the TEM image show that all nanoparticles were present in the monodisperse stage.

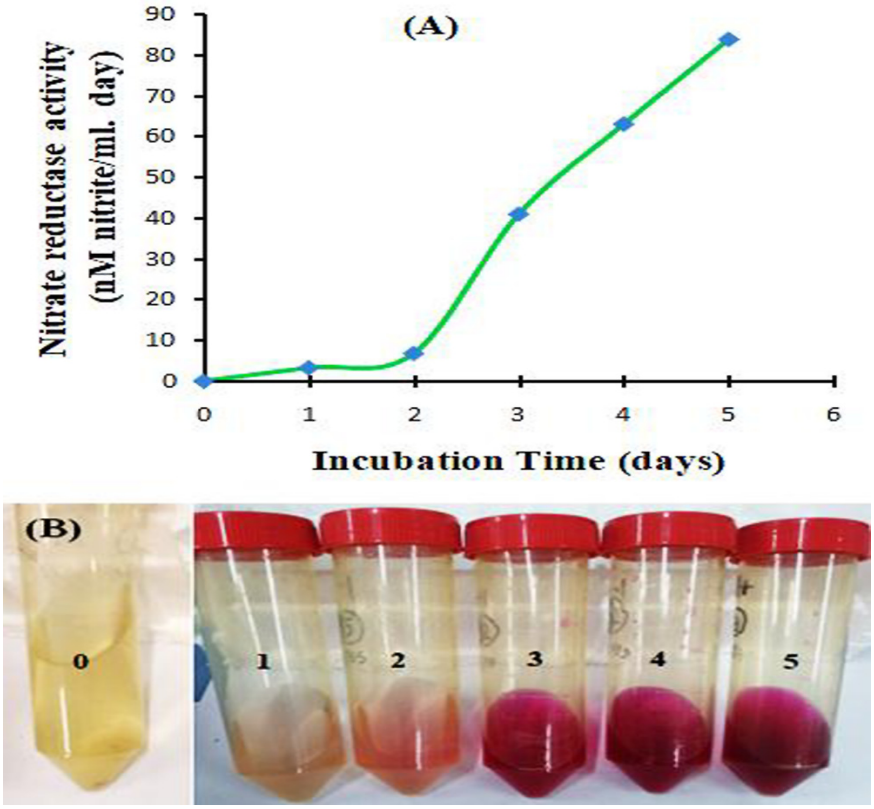

Fig. 5. Reductase enzyme activity (A) and observed assay results (B) of the fungal cell-free filtrate of *Aspergillus niger* DS22 (ON076463.1) under incubation for (1-5 days)

Angle	Mean (nm)	P.I.	Diff.Coef (m^2/s)	Counts/s	Baseline Error	Overflow
11.1°	17.3	-12.022	4.51e-11	2.24e+06	0.52%	0
15.8°	35.2	-1.723	2.21e-11	1.35e+06	0.49%	0

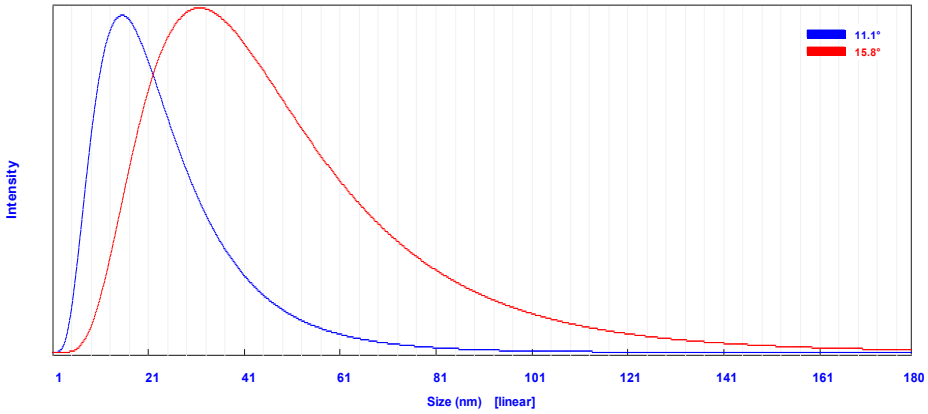

Fig. 6. Particle size analyzer of TiO_2NPs biosynthesized by *Aspergillus niger* DS22 (ON076463.1) cell-free filtrate under all optimized conditions

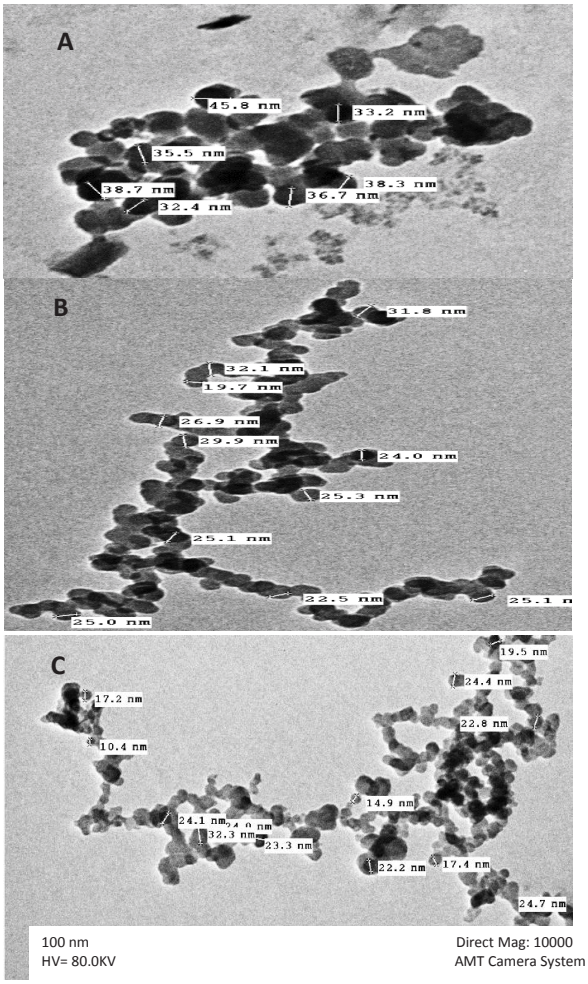

Fig. 7. TEM images of TiO_2NPs biosynthesized by *Aspergillus niger* DS22 (ON076463.1) cell-free filtrate under all optimized conditions

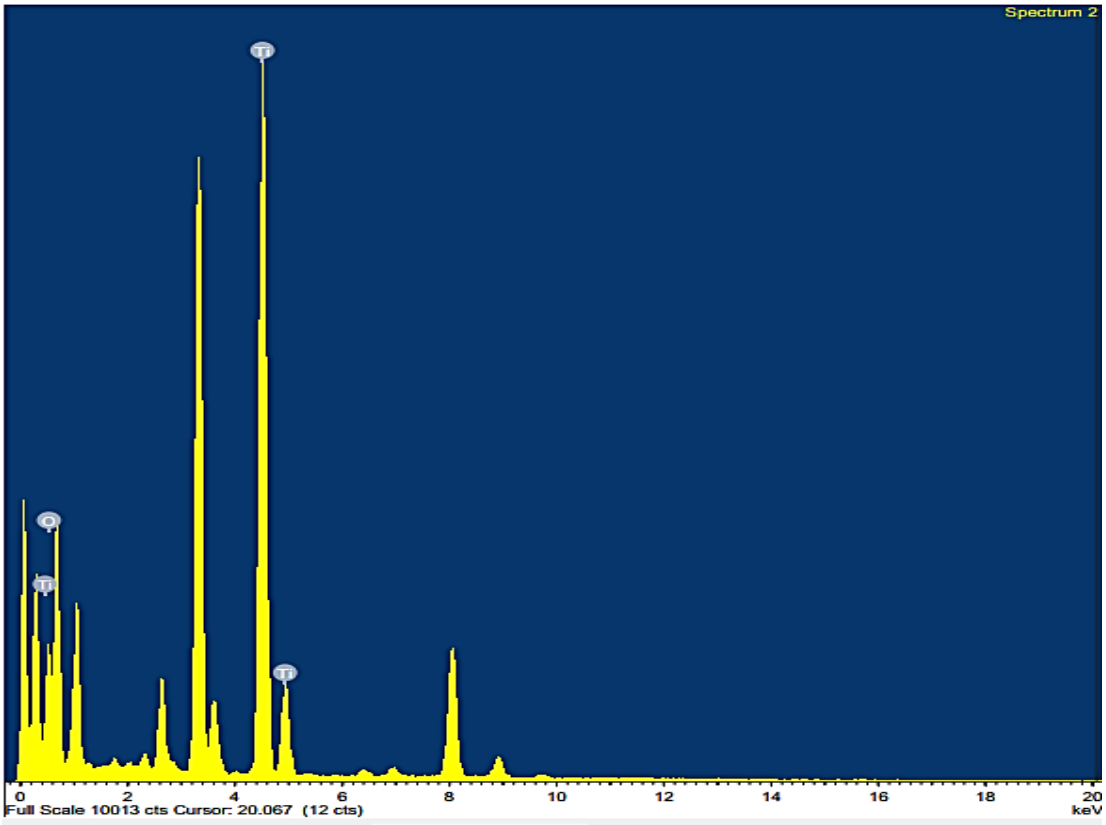

Fig. 8. EDX analysis of TiO_2NPs synthesized by *Aspergillus niger* DS22 (ON076463.1) cell-free filtrate under all optimized conditions

Fourier transform infrared spectroscopy (FTIR) analysis

The Fourier transform infrared spectroscopy spectrum (FTIR) of the titanium dioxide nanoparticles was illustrated in Fig. 9. Both chemical and microbiological TiO_2NPs exhibit the distinctive signal caused by the vibration of the Ti-O-Ti bond at 450-900cm^{-1} (Wahyuni et al., 2017). In the present study, FTIR analysis of TiO_2NPs had a distinctive band which was observed at 522.70cm^{-1} can be attributed to the Ti-O-O stretching vibration. Bands at 810.16 cm^{-1} and 881.81 cm^{-1} correspond to the presence of Ti-O stretching of Ti-O-Ti bonds. At 3390.96cm^{-1} a wide band is seen. This signal relates to the O-H stretching, which indicates that water molecules were involved since TiO_2NPs were exposed to air during sample processing (Wang, 2007). The peaks around 2924.47cm^{-1} are assigned to the symmetric stretch (C–H) of the CH_2 and CH_3 groups of aliphatic chains. The broad band observed in 1648.69 cm^{-1} and 1745.38 cm^{-1} indicated the presence of amide I and amide II bonds which could suggest the involvement of extracellular protein in the synthesis of nanoparticles (Rangnekar et al., 2007). In 1553.84cm^{-1}, 1455.29cm^{-1} and 1413.50 cm^{-1} the typical signals of C = O and N-H vibrations due to the existence of amine and amide groups are displayed. The peak at 1239.76 correlated to the vibrations of the C-O stretch, possibly due to the existence of a carboxylic acid or an alcohol group. The band at 1074.53cm^{-1} met the vibrations of the C-N stretching of aliphatic amines. The peaks at 1553.84cm^{-1} and 1413.50cm^{-1} might also indicate the C= C ring stretching and bending vibration of CH_2. The whole of signals can be imputable to the presence of bioactive molecules like carbohydrates or peptides seamed to the TiO_2NPs bio-fabricated by *Aspergillus niger* DS22 (ON076463.1) FTIR spectra revealed the respective metal as well as the peak for fungal protein. These biomolecules with different functional groups could facilitate the nanoparticles' nucleation and play a role in the biosynthesis process acting as capping and stabilizing agents making TiO_2 nanoparticles more stable and eco-friendlier (Abdel-Kareem et al., 2021). Similar studies explained by Tarafdar et al. (2013) and Rajakumar et al. (2012) for the fungus-mediated synthesis of TiO_2 nanoparticles supported the characteristic details of FTIR spectra.

X-ray diffraction (XRD)

The XRD pattern of commercial TiO_2 and those biosynthesized using fungal biomass-free filtrate of *Aspergillus niger* DS22 (ON076463.1) was shown in (Supplementary Materials Fig. S9 and 10) correspondingly. A high-pitched diffraction peak was noticed in commercial TiO_2 while the biosynthesized TiO_2 nanoparticles had no distinct sharp but continuous broadening to include all the sharp and distinct peaks present in commercial TiO_2 with less intensity.

The measurements of (XRD) were conducted over the diffraction angle (2) 10◦–80◦. The XRD pattern revealed intense peaks at 25.296°, 37.835°, 48.080°, 53.927°, 55.104° and 62.725°. These intense peaks correspond to (101), (004), (200), (105), (211), and (204) when matched to the JCPDS (No. 99-101-0954), that is considered as a descriptive measure of biologically generated TiO_2NPs crystallites, Bragg's reflection was determined to be the Anatase type. The existence of microbial proteinaceous residues related to crystalline TiO_2NPs was reflected by a line broadening of the spectrum peaks and a slight shift in peak positions from XRD and a small background at 2 range 20-30. The sizes of the crystallite were determined by the using the Scherrer formula to the principal intense peaks and proved to be in the 26nm range. The current study's findings were consistent with those of Hassan et al. (2020). These results were also in agreement with Sankar et al. (2014) who recorded that, XRD analysis patterns in their study lacked distinct diffraction peaks, proposing that biosynthesized TiO_2NPs are amorphous in nature.

Biomedical application of TiO_2NPs synthesized by Aspergillus niger DS22 (ON076463.1)

Antibacterial activity

The antibacterial efficacy of TiO_2NPs was illustrated in (Table 4, and Fig. 10). The results indicated that the biosynthesized TiO_2NPs had antibacterial strength toward the five tested pathogenic bacterial strains and the maximum activity was against MRSAATCC25923 (34mm inhibition zone) and minimum activity was against Klebsiella pneumoniaATCC700603 (19.66mm inhibition zone). The antibacterial impact can be linked to the generation of reactive oxygen species, which resulted in phospholipid peroxidation through decreasing adhesion and changing the ionic balance (Tiquia-Arashiro & Rodrigues, 2016). TiO_2 nanoparticles inhibit respiratory cytosolic enzymes and modify macromolecule structures, resulting in cellular integrity and gene expression, followed by cell death (Ovais et al., 2018; Sagadevan et al., 2022). Results in the present study agreed with Thakur et al. (2019) who found that Titanium dioxide nanoparticles showed maximum activity against *E. coli* and *Klebsiella pneumonia* with inhibition zone diameters 27.67 ± 0.76mm and 20.67 ± 1.45mm, respectively at 200µg/mL. Similar results were observed with Ali et al. (2022) who noted that the TiO_2 nano compound exerted promising antibacterial activity against *Bacillus subtilis, Escherichia coli,* and *Cryptococcus neoformans,* showing minimum inhibitory concentrations (MIC) of 15.62, 62.5 and 7.81µg/mL, respectively. Also, Akinola et al. (2020) found that TiO_2 nanoparticles had antibacterial potential against *Escherichia coli* and *Klebsiella pneumoniae* gained from the urine, Staphylococcus aureus gained from pus and *Pseudomonas aeruginosa* gained from the wound.

Evaluation of the wound healing activities of TiO_2NPs biosynthesized by Aspergillus niger DS22 (ON076463.1)

In the present work, dermal cell lines were treated with TiO_2NPs biosynthesized by *Aspergillus niger* DS22 (ON076463.1) to assess the cellular healing and, consequently, TiO_2 nanoparticle's efficacy to control wounds at evident times. As shown in Fig. 11A, from wound initiation date (day 0) to 48h, the cell-free areas were nearly closed by 65.96% in comparison with the control 58.49%. Also, wound terminating in dermal cell lines cells handled with Titanium dioxide nanoparticles biosynthesized by *Aspergillus niger* DS22 judged to control was explained in Fig. 11B and the cell migration rate (in micrometer per hour) is represented in Fig. 11C. Titanium dioxide nanoparticles showed significant wound-healing action in vitro after 24h. than the control. Sivaranjani & Philominathan (2016) reported similar results for titanium dioxide nanoparticles green synthesized by using *Moringa oleifera* leaves. Also, Hassan et al. (2020) recorded that fungal-mediated titanium dioxide nanoparticles had a significant degree of wound-healing activity.

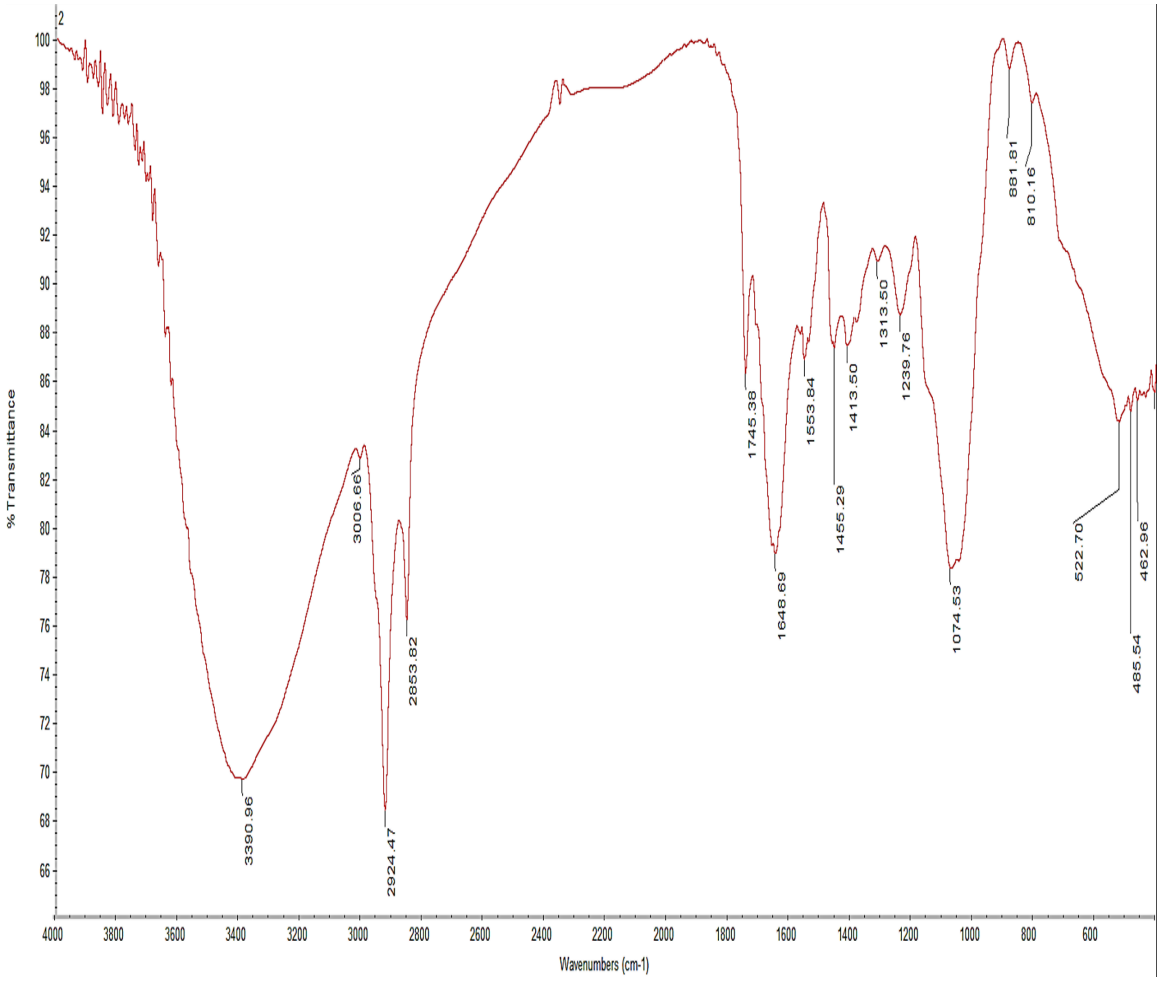

Fig. 9. FTIR spectrum of TiO_2 nanoparticles biosynthesized by *Aspergillus niger* DS22 (ON076463.1) in the range of 400–4000cm^{-1}

TABLE 4. Determination of antibacterial activity of biosynthesized TiO_2NPs against some pathogenic bacterial strains

Pathogenic bacteria	Antibacterial activity (Inhibition zone mm)			
	Fungal free filtrate	Ti^4 salt sol.	TiO_2NPs	Antibacterial standard (Amoxycillin 85µg /0.1mL)
Klebsiella pneumonia ATCC700603	-ve	-ve	19.66	18.33
Pseudomonas aeruginosa ATCC27853	-ve	9	22.33	24
E. coli ATCC25922	-ve	-ve	22.5	**23.5**
MSSA ATCC25923	-ve	-ve	28.33	26.66
MRSA ATCC25923	-ve	-ve	34	37.66

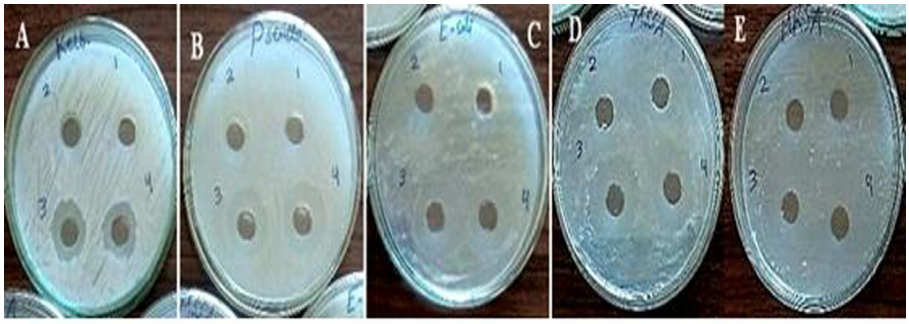

Fig. 10. Antibacterial activity of biosynthesized TiO_2NPs against some pathogenic bacterial strains (A): *Klebsiella pneumonia* (ATCC700603); (B): *Pseudomonas aeruginosa* (ATCC27853); (C): *Escherichia coli* (ATCC25922); (D): Methicillin Sensitive *Staphylococcus aureus* (MSSA ATCC25923) and (E): Methicillin-Resistant *Staphylococcus aureus* (MRSA ATCC43300) ((1) Fungal free filtrate; (2) Ti^{+4} Salt Sol.; (3) TiO_2NPs (75µg/0.1mL; (4) Antibacterial standard; Amoxycillin (85µg/0.1mL)

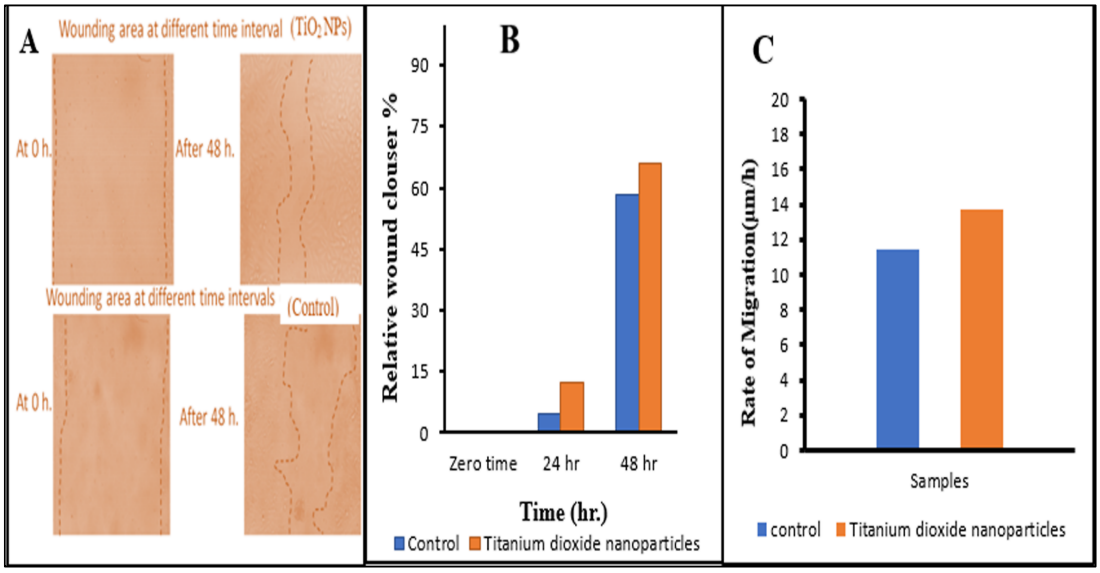

Fig. 11. (A) The wound healing activity of TiO_2NPs synthesized by *Aspergillus niger* DS22 (ON076463.1) (B) determination of wound closure in epidermal cell line using TiO_2NPs against a control. (C) cell migration rates (µm/h)

Evaluation of Anti-inflammatory activities of TiO_2NPs

The Anti-inflammatory activity of TiO_2NPs biosynthesized by *Aspergillus niger* DS22 (ON076463.1) in this study was tested, represented graphically in Fig. 12, Supplementary Materials Fig. S11 and Supplementary Materials Table S4. Results clarified that TiO_2NPs displayed inhibition of human erythrocyte hematolysis of 69%, 75.9%, 83.9%, 87.4%, 95.2%, and 97.7% at concentrations of 100, 200, 400, 600, 800 and 1000µg/mL compared to inhibition by standard Indomethacin with 91.6%, 92.5%, 93.4%, 94.6, 96.2 and 98.6% at the same concentrations, respectively. These results were in complete agreement with those of Chahardoli et al. (2022) who used TiO_2NPs biosynthesized by caffeic acid with an average particle size of 23.6nm and found that these particles had no hemolytic effects had good membrane stabilizing activity and inhibited protein denaturation, just like the reference medication. Some studies reported that titanium dioxide nanoparticles have potent anti-inflammatory potentials after incubation with blood by reducing platelet counts (Seisenbaeva et al., 2017; Sonmez & Sonmez, 2017). As per studies, TiO_2NPs are known to increase thrombin-antithrombin (TAT) levels, i.e. more thrombin inactivation by antithrombin takes place, and subsequently, inflammation is reduced by suppressing the Protease-Activated Receptor (PAR) pathway (Seisenbaeva et al., 2017; Agarwal et al., 2019).

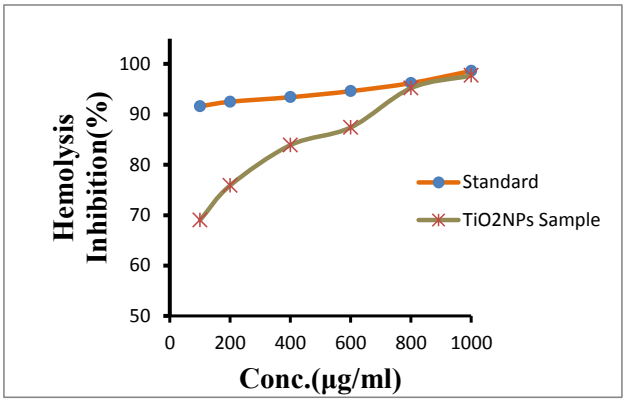

Fig. 12. Anti-inflammatory activity of TiO_2NPs biosynthesized by *Aspergillus niger* DS22 (ON076463.1) compared with standard Indomethacin at the same concentrations

Conclusion

In conclusion, an eco-friendly green approach was utilized to produce TiO_2NPs synthesized by the fungal cell-free filtrate of *Aspergillus niger* DS22 (ON076463.1). The Results of our study evoked the ability of *Aspergillus niger* DS22 (ON076463.1) filtrate to build up TiO_2NPs in a spherical shape and dispersed without aggregation with a size average of 26.619±7.577nm. Based on the information reported herein, it is possible to infer that biosynthesized TiO_2NPs can be used as an alerted and effective potential antibacterial mediator alongside several human pathogenic bacteria. This study proves the efficacy of TiO_2NPs in closing wounds in dermal cells by (65.96%) compared with control (58.49%) in 48h. The presence of numerous beneficial metabolites has been identified by gas chromatography-mass spectrometry (GC-MS) analysis, nearly all of which are accountable for the extract's anti-inflammatory and antibacterial effects. Overall, TiO_2NPs produced by *Aspergillus niger* DS22 (ON076463.1) show various advantageous features and might be considered as a potential novel ingredient in pharmaceutical products.

Availability of data: This investigation offers all the data collected or estimated throughout this work.

Conflict of interest: All authors proclaim that there is no conflict of interest.

Authors' contribution: Enayat M. Desouky, Sawsan AbdEllatif, Nermine N. Abed, and Amira Y. Mahfouz constructed the framework and helped in the practical work, data representation, writing, reviewing, and editing. Dalia K. Abd El Hamid the PhD student who did the practical work and participated in the writing.

Ethical approval: Not applicable.

References

Abbas, M., Holmes, A., Price, J. (2020) Surgical site infections following elective surgery. *The Lancet Infectious Diseases*, **20**, 898–899.

AbdElmohsen, S. (2020) Biosynthesis of some nanoparticles for the application in the treatment of contaminated drinking water. *Ms.D. Dissertation,* Al-Azhar University, Cairo, Egypt.

Abdel-Kareem, M.M., Zohri, A.A., Rasmey, A. M.(2021) Biosynthesis of silver nanoparticles by *Aspergillus sakultaeiannsis* and its antibacterial activity against human pathogens. *Egyptian Journal of Microbiology*, **56**, 11-24.

Abdel-Wahhab, M.A., El-Nekeety, A.A., Hathout, A. S., Salman, A.S., Abdel-Aziem, S.H., et al. (2020) Bioactive compounds from *Aspergillus niger* extract enhance the antioxidant activity and prevent the genotoxicity in aflatoxin B1-treated rats. *Toxicon*, **181**, 57-68.

Abdullah, N.A., Hashim, N.F.M., Ammar, A., Zakuan, N.M. (2021) An insight into the anti-angiogenic and anti-metastatic effects of oridonin: Current knowledge and future potential. *Molecules (Basel, Switzerland)*, **26**(4), 775. http://dx.doi.org/10.3390/molecules26040775. PMid:33546106.

Agarwal, H., Nakara, A., Shanmugam, V.K. (2019)

Anti-inflammatory mechanism of various metal and metal oxide nanoparticles synthesized using plant extracts: A review. *Biomedicine & Pharmacotherapy*, **109**, 2561-2572.

Ahmed, N.E. Salem, S.S., Hashem, A.H. (2022) Statistical optimization, partial purification, and characterization of phytase produced from Talaromyces purpureogenus nsa20 using potato peel waste and its application in dyes de-colorization. *Biointerface Research in Applied Chemistry*, **12**(4), 4417–4431.

Akinola, P.O., Lateef, A., Asafa, T.B., Beukes, L.S., Hakeem, A.S., Irshad, H.M. (2020) Multifunctional titanium dioxide nanoparticles biofabricated via phytosynthetic route using extracts of *Cola nitida:* Antimicrobial, dye degradation, antioxidant and anticoagulant activities. *Heliyon*, **6**, 1-9.

Al-Garni, S., Ghanem, K., Bahobail, A. (2009) Biosorption characteristics of *Aspergillus fumigates* in removal of cadmium from an aqueous solution. *African Journal of Biotechnology*, **8**(17), 4163-4172.

Ali, O.M., Hasanin, M.S., Suleiman, W.B., Helal, E.E., Hashem, A.H., (2022) Green biosynthesis of titanium dioxide quantum dots using watermelon peel waste: Antimicrobial, antioxidant, and anticancer activities. *Biomass Conversion and Biorefinery*. https://doi.org/10.1007/s13399-022-02772-y

Amin, B.H., Ahmed, H.Y., El Gazzar, E.M., Badawy, M.M.M. (2021) Enhancement the Mycosynthesis of Selenium nanoparticles by using gamma radiation. *Dose-Response: An International Journal*, **19**(4) 1–8.

Anosike, C.A., Obidoa, O., Ezeanyika, L.U. (2012) Membrane stabilization as a mechanism of the anti-inflammatory activity of methanol extract of garden egg (*Solanum aethiopicum*). *Journal of Pharmaceutical Sciences*, **20**, 76.

Atta, H.M., Refaat, B.M., El-Waseif, A.A. (2009) Application of biotechnology for production, purification and characterization of peptide from *P. aeruginosa. World Journal of Microbiology and Biotechnology,* **35**, 208-215.

Avilala, J., Golla, N. (2019) Antibacterial and antiviral properties of silver nanoparticles synthesized by marine actinomycetes. *International Journal Pharmaceutical Sciences and Research (IJPSR),* **10**(3), 1223-1228.

Bai, J., Zhang, Y., Tang, C., Hou, Y., Ai, X., Chen, X., et al. (2021) Gallic acid: Pharmacological activities and molecular mechanisms involved in inflammation related diseases. *Biomedicine and Pharmacotherapy Journal*, **133**, 110985.

Bose, D., Chatterjee, S. (2016) Biogenic synthesis of silver nanoparticles using guava (*Psidium guajava*) leaf extract and its antibacterial activity against *Pseudomonas aeruginosa*. *Applied Nanoscience*, **6**, 895–901.

Chahardoli, A., Farshad Qalekhani, F., Shokoohinia, Y., Fattahi, A. (2022) Caffeic acid-based titanium dioxidenanoparticles: Blood compatibility, anti-inflammatory, and cytotoxicity. *Journal of Molecular Liquids*, **361**, 119674. https://doi.org/10.1016/j.molliq.2022.119674

Cormier, N., Yeo, A., Fiorentino, E., Paxson, J. (2015) Optimization of the wound scratch assay to detect changes in murine mesenchymal stromal cell migration after damage by soluble cigarette smoke extract. *Journal of Visualized Experiments*, **106**, e53414, 1-9. https:// doi. org/ 10. 3791/ 53414

Durairaj, B., Xavier, T., Muthu, S. (2014) Research article fungal generated titanium dioxide nanoparticles: A potent mosquito (*Aedes aegypti*) larvicidal agent. *Scholars Academic Journal of Bioscience,* **2**(9), 651–658.

El-Baba, C., Baassiri, A., Kiriako, G., Dia, B., Fadlallah, S., Moodad, S., Darwiche, N. (2021) Terpenoids' anti-cancer effects: Focus on autophagy. *Apoptosis*, **26**(9-10), 491-511.

Elbestawy, M.K.M., El-Sherbiny, G.M., Moghannem, S.A. (2023) Antibacterial, antibiofilm and anti-Inflammatory activities of eugenol clove essential oil against resistant *Helicobacter pylori. Molecules*, **28**, 2448. https://doi.org/10.3390/molecules28062448

Ellatif, S., Abed, N.N., Mahfouz, A. Y., Desouky, E.M., Abd El Hamid, D.K. (2021) Production, purification, and identification of glycine, N-(m-anisoyl)-methyl ester from *Pseudomonas aeruginosa* with antimicrobial and anticancer activities. *Kuwait Journal of Science*, **48**(3),1-12.

Ellatif, S.A., Abdel Razik,E.S., AL-surhanee, A.A., Al-

Sarraj, F., Daigham, G.E., Mahfouz, A.Y. (2022) Enhanced production, cloning, and expression of a xylanase gene from endophytic fungal strain *Trichoderma harzianum* kj831197.1: Unveiling the *in vitro* anti-fungal activity against phytopathogenic fungi. *Journal of Fungi,* **8**, 447. https://doi.org/10.3390/jof8050447

Elsayed, A., El-Shamy, G.M., Attia, A.A. (2022) Biosynthesis, characterization, and assessment of Zirconia nanoparticles by *Fusarium oxysporum* species as potential novel antimicrobial and cytotoxic agents. *Egyptian Journal of Botany,* **62**(2), 507-522.

Elsehemy, I.A., El Deen, A.M.N., Awad, H.M., Kalaba, M.H., Moghannem, S.A., Tolba, I.H., Farid, M.A. (2020) Structural, physical characteristics and biological activities assessment of scleroglucan from a local strain *Athelia rolfsii* TEMG, International *Journal of Biological Macromolecules*, **163**, 1196-1207.

Eltarahony, M., Ibrahim, A., El-shall, H., Ibrahim, E., Althobaiti, F., Fayad, E. (2021) Antibacterial, antifungal and antibiofilm activities of silver nanoparticles supported by crude bioactive metabolites of bionanofactories isolated from Lake Mariout. *Molecules*, **26**, 3027.

Flowers, L., Grice, E.A. (2020) The skin microbiota: Balancing risk and reward. *Cell Host and Microbe,* **28**, 190–200.

Fushimi, T., Inui, S., Nakajima, T., Hosokawa, K., Ogasawara, M., Itami, S. (2012) Green light emitting diodes accelerate wound healing: Characterization of the effect and its molecular basis *in vitro* and *in vivo. Wound Repair Regeneration*, **20**(2), 226–235.

Gini, T.G., Jeya Jothi, G. (2018) Column chromatography and HPLC analysis of phenolic compounds in the fractions of *Salvinia molesta* Mitchell. *Egyptian Journal of Basic and Applied Science,* **5**, 197–203.

Gowri, M., Ananthalakshmi, S., Therese Punitha, J. (2013) *In-vitro* antimicrobial screening of naphthalene acetic acid compounds. *International Journal of Pharmacy & Life Sciences*, **4**(7), 2780-2784.

Hackl, E., Zechmeister, S. Bodroosy, L., Sessitsch, A. (2004) Comparison of diversities and composition of bacterial population inhabiting nature forestsoils. *Applied and Environmental Microbiology,* **70**, 5057-5065.

Hamedi, S., Shojaosadati, S.A., Shokrollahzadeh, S., Hashemi Najafabadi, S. (2013) Extracellular biosynthesis of silver nanoparticles using a novel and nonpathogenic fungus, Neurospora intermedia: Controlled synthesis and antibacterial activity. *World Journal of Microbiology and Biotechnology,* **30**, 693–704.

Hassan, H., Omoniyi, K.I., Okibe, F.G., Nuhu, A.A., Echioba, E.G., Egwim, E.C. (2020) Assessment of wound healing activity of green synthesized titanium oxide nanoparticles using *Strychnos spinosa* and *Blighia sapida*. *Journal of Applied Science and Environmental Management*, **24**(2), 197-206.

Ikram, M., Javed, B., Hassan,S.W., Satti, S.H., Sarwer, A., Raja, N.I., Zia-ur-Rehman, M.Z. (2021) Therapeutic potential of biogenic titanium dioxide nanoparticles: A review on mechanistic approaches. *International Journal of Nanomedicine,* **16**(1), 1-19.

Javed, B., Nawaz, K., Munazir, M. (2020) Phytochemical analysis and antibacterial activity of tannins extracted from *Salix alba* L. against different gram-positive and gram-negative bacterial strains. *Iranian Journal of Science and Technology, Transaction A: Science*, **44**, 1303–1314.

Jha, A.K., Prasad, K., Kulkarni, A. (2009) Synthesis of TiO_2 nanoparticles using microorganisms. *Colloids and Surfaces B- Biointerfaces,* **71**, 226–229.

Kim, H., Jeon, D., Oh, S., Nam, K., Son, S., Chan Gye, M. Shin, I. (2019) Titanium dioxide nanoparticles induce apoptosis by interfering with EGFR signaling in human breast cancer cells. *Environmental Research*, **175**, 117–123.

Laemmli, U.K. (1970) Cleavage of structural proteins during the assembly of the head bacteriophage. *Nature*, **14**(227), 680– 685.

Lowry, O.H., Rosenbrough, N.J, Farr, A.L., Randall, R.J. (1951) Protein measurement with the Folin Phenol Reagent. *Journal of Biological Chemistry,* **193**, 265-275.

Mashraqi, A., Modafer, Y., Al Abboud, M.A., Salama, H.M., Abada, E. (2023) HPLC analysis and

molecular Docking study of *Myoporum serratum* seeds extract with its bioactivity against pathogenic microorganisms and cancer cell lines. *Molecules*, **28**, 4041. https://doi.org/10.3390/molecules28104041

McClenny, N. (2005) Laboratory detection and identification of *Aspergillus* species by microscopic observation and culture. *Journal of Medical Mycology,* **43**(1), S125-S128.

Mohamed, A.A., Fouda, A., Abdel-Rahman, M.A., Hassan, S.E., El-Gamal, M.S., Salem, S.S., Shaheen, T.I. (2019) Fungal strain impacts the shape, bioactivity and multifunctional properties of green synthesized zinc oxide nanoparticles. *Biocatalysis and Agricultural Biotechnology,* **19**, 101103.

Mokhtar, F.Y., Abo-El Nasr, A., Elaasser, M.M., Elsaba, Y.M. (2023) Bioactive secondary metabolites from *Aspergillus fumigatus* ON428521 isolated from Wadi El Rayan, El Fayum Governorate. *Egyptian Journal of Botany*, **63**(1), 233-250.

Muhammad, N., Akbar, A., Abbas, G., Hussain, M., Khan, T.A. (2015) Isolation, optimization and characterization of antimicrobial peptide producing bacteria from soil. *Journal of Animal and Plant Science,* **25**(4), 1107-1113.

Mukherjee, K., Gupta, R., Kumar, G., Kumari, S., Biswas, S., Padmanabhan, P. (2018) Synthesis of silver nanoparticles by *Bacillus clausii* and computational profiling of nitrate reductase enzyme involved in production. *Journal of Genetic Engineering Biotechnology*, **16**, 527–536.

Nabi, G., Aain, Q.U., Khalid, N.R., Tahir, M.B., Rafique, M., et al. (2018) A review on novel eco-friendly green approach to synthesis TiO_2 nanoparticles using different extracts. *Journal of Inorganic and Organometallic Polymers and Materials*, **28**, 1552–1564.

Nasr, R., Hasanzadeh, H., Khaleghian, A., Moshtaghian, A., Emadi, A., Moshfegh, S. (2018) Induction of apoptosis and inhibition of invasion in gastric cancer cells by titanium dioxide nanoparticles. *Oman Medical Journal,* **33**(2), 111–117.

Naz, S.A., Jabeen, N., Sohail, M., Rasool, Sh.A. (2015) Biophysico chemical characterization of Plocin SA189 produced by *Pseudomonas aeruginosa* SA189. *Brazilian Journal of Microbiology,* **46**(4), 1147-1154.

Niero, E.L.d.O., Machado-Santelli, G.M. (2013) Cinnamic acid induces apoptotic cell death and cytoskeleton disruption in human melanoma cells. *Journal of Experimental and Clinical Cancer Research,* **32**, 31.

Ottoni, C.A., Simões, M.F., Fernandes, S., Gomes dos Santos, J., Sabino da Silva, E., Brambilla de Souza, R.F., Maiorano, A.E. (2017) Screening of filamentous fungi for antimicrobial silver nanoparticles synthesis. *AMB Express,* **7**, 31-41.

Ovais, M., Khalil, A.T., Ayaz, M., Ahmad, I., Nethi, S.K., Mukherjee, S. (2018) Biosynthesis of metal nanoparticles via microbial enzymes: Amechanistic approach. *International Journal of Molecular Science,* **19**(12), 4100.

Rajakumar, G., Rahuman, A.A., Roopan, S.M., Khanna, V.G., Elango, G., Kamaraj, C., Zahir, A.A., Velayutham, K. (2012) Fungus-mediated biosynthesis and characterization of TiO_2 nanoparticles and their activity against pathogenic bacteria. *Spectrochimica Acta Part A: Molecular and Biomolecular Spectroscopy*, **91**, 23-29.

Raliya, R., Tarafdar, J. (2015) Biosynthesis and characterization of zinc, magnesium and titanium nanoparticles: An eco-friendly approach. *International Nano Letters*, **4**(1), 1-10.

Raliya, R. Rathore, I., Tarafdar, J.C. (2013) Development of microbial nanofactory for zinc, magnesium, and titanium nanoparticles production using soil fungi. *Journal of Bionanoscience*, **7**, 1–7.

Raliya, R., Biswas, P., Tarafdar, J.C. (2015) TiO_2 nanoparticle biosynthesisand its physiological effect on mung bean (*Vigna radiata* L.). *Biotechnology Reports*, **5**, 22–26.

Rangnekar, A., Sarma, T., Singh, A., Deka, J., Ramesh, A., Chattopadhyay, A. (2007) Retention of enzymatic activity of α- amylase in the reductive synthesis of gold nanoparticles. *Langmuir Book,* **23**(10), 5700-5706.

Rathore, C., Yadav, V.K., Gacem, A., AbdelRahim, S.K.,Verma, R.K., Chundawat, R.S., et al. (2023) Microbial synthesis of titanium dioxidenanoparticles and their importance in waste water treatment and antimicrobial activities: A review. *Frontiers in Microbiology*, **14**, 1270245. doi: 10.3389/fmicb.2023.1270245

Rocha, K.C., Alonso, C.G., Leal, W.G.O., Schultz, E.L., Andrade, L.A., Ostroski, I.C. (2020) Slow pyrolysis of *Spirulina platensis* for the production of nitrogenous compounds and potential routes for their separation. *Bioresource Technology,* **313**, 123709. https://doi.org/10.1016/j.biortech.2020.123709

Roy, S., Santra, S., Das, A., Dixith , S., Sinha, M. Ghatak, S., Ghosh, N. et al. (2020) *Staphylococcus aureus* biofilm infection compromises wound healing by causing deficiencies in granulation tissue collagen. *Annals of Surgery,* **271**, 1174–1185.

Sagadevan, S., Imteyaz, S., Murugan, B., Lett, J. A., Sridewi, N., et al. (2022) A comprehensive review on green synthesis of titanium dioxide nanoparticles and their diverse biomedical applications. *De GRUYTER, Green Processing and Synthesis*, **11**, 44–63.

Salau, V.F., Erukainure, O.L., Ibeji, C.U., Olasehinde, T.A., Koorbanally, N.A., Islam, M.S. (2020) Vanillin and vanillic acid modulate antioxidant defense system via amelioration of metabolic complications linked to Fe^{2+}-induced brain tissues damage. *Metabolic Brain Disease*, **35**, 727–738.

Salem, S.S. (2023) A mini review on green nanotechnology and its development in biological effects. *Archives of Microbiology,* **205**, 128,1-15.

Salem, S.S., Fouda, A. (2021) Green synthesis of metallic nanoparticles and their prospective biotechnological applications: An overview. *Biological Trace Element Research,* **199**(1), 344–370.

Sankar, R., Dhivya, R., Shivashangari, K.S., Ravikumar, V. (2014) Wound healing activity of *Origanum vulgare* engineered titanium dioxide nanoparticles in Wistar Albino rats. *Journal of Materials Science: Materials in Medicine*, **25**, 1701–1708.

Scimeca, M., Bischetti, S., Lamsira, H., Bonfiglio, R., Bonanno, E. (2018) Energy dispersive X-ray (EDX) microanalysis: A powerful tool in biomedical research and diagnosis. *European Journal of Histochemistry,* **62**(1), 1-10.

Seisenbaeva, G.A., Fromell, K., Vinogradov, V.V., Terekhov, A.N., Pakhomov, A.V., Nilsson, B., Ekdahl, K.N., Vinogradov, V.V., Kessler, V.G. (2017) Dispersion of TiO_2 nanoparticles improves burn wound healing and tissue regeneration through specific interaction with blood serum proteins. *Scientific Reports,* **7**, 15448, 10.1038/s41598-017-15792-w

Selim, M.T., Salem, S.S., Mohamed, A.A., El-Gamal, M.S., Awad, M.F., Fouda, A. (2021) Biological treatment of real textile effluent using *Aspergillus flavus* and *Fusarium oxysporium* and their consortium along with the evaluation of their phytotoxicity. *Journal of Fungi*, **7**(3), 193.

Sharaf, M.H., Nagiub, A., Salem, S.S., Kalaba, M., El-Fakharany, E., Abd El-Wahab, H. (2022) A new strategy to integrate silver nanowires with waterborne coating to improve their antimicrobial and antiviral properties. *Pigment & Resin Technology*, (ahead-of-print). DOI:10.1108/PRT-12-2021-0146.

Shinde, U.A., Phadke, A.S., Nair, A.M., Mungantiwar, A.A., Dikshit, V.J., Sarsf, M.N. (1989) Membrane stabilization activity- a possible mechanism of action for the anti-inflammatory activity of *Cedrus deodara* wood oil. *Fitoterapia*, **70**, 251–257.

Sivaranjani, V., Philominathan, P. (2016) Synthesize of Titanium dioxide nanoparticles using *Moringa oleifera* leaves and evaluation of wound healing activity. *Journal of Wound Medicine,* **12**, 1-5.

Soliman, M.I., Mohammed, N.S., EL-Sherbeny, G., Safhi, F.A., ALshamrani, S.M., et al. (2022) Antibacterial, antioxidant activities, GC-mass characterization, and cyto/genotoxicity effect of green synthesis of silver nanoparticles using latex of *Cynanchum acutum* L. *Plants*, **12**, 172. https://doi.org/ 10.3390/plants12010172

Soliman, S.A., Hafez, E.E., Al-Kolaibe, A.M.G., Abdel Razik,E.S.S., Abd-Ellatif, S., Ibrahim, A.A., et al. (2023) Biochemical characterization, antifungal activity, and relative gene expression of two mentha essential oils controlling *Fusarium oxysporum,* the causal agent of *Lycopersicon esculentum* root rot. *Plants*, **11**, 189. https://doi.org/ 10.3390/plants11020189

Sonmez, O., Sonmez, M. (2017) Role of platelets in immune system and inflammation. *Porto Biomedical Journal*, **2**, 311- 314.

Spagnoletti, F.N., Spedalieri, C., Kronberg, F., Giacometti, R. (2019) Extracellular biosynthesis of bactericidal Ag/AgCl nanoparticles for crop

protection using the fungus *Macrophomina phaseolina. Journal of Environmental Management,* **231**, 457–466.

Striet, W., Schmitz, R. (2004) Metgenomics the key to the uncultured microbes. *Current Opinion in Microbiology,* **17**, 492-498.

Subbaiya, R., Saravanan, M., Priya, A.R., Shankar, K.R., Selvam, M., et al. (2017) Biomimetic synthesis of silver nanoparticles from *Streptomyces atrovirens* and their potential anticancer activity against human breast cancer cells. *IET Nanobiotechnology,* **11**, 965–972.

Tarafdar, A., Raliya, R., Wang, W., Biswas, P., Tarafdar, J. (2013) Green synthesis of TiO_2 nanoparticle using *Aspergillus tubingensis. Advanced Science, Engineering and Medicine,* **5**(9), 943-949.

Thakur, B.K., Kumar, A., Kumar, D. (2019) Green synthesis of titanium dioxide nanoparticles using *Azadirachta indica* leaf extract and evaluation of their antibacterial activity. *South African Journal of Botany*, **124**, 223–227.

Tiquia-Arashiro, S., Rodrigues, D. (2016) "*Extremophiles: Applications in Nanotechnology*", Springer International Publishing AG, pp. 163-193. DOI 10.1007/978-3-319-45215-9_5

Ullah, R., Ikram, M., Park, T.J., Ahmad, R., Saeed, K., Alam, S.I., et al. (2020) Vanillic acid, a bioactive phenolic xompound, xounteracts LPS-induced neurotoxicity by regulating c-Jun N-terminal kinase in mouse brain. *International Journal of Molecular Science*, **22**, 361.

Verma, V., Al-Dossari, M., Singh, J., Rawat, M., Kordy, M.G.M., Shaban, M. (2022) A review on green synthesis of TiO_2 NPs: Photocatalysis and antimicrobial applications. *Polymers*, **14**, 1444.

Wang, L. (2017) The antimicrobial activity of nanoparticles: present situation and prospects for the future. *International Journal of Nanomedicine,* **12**, 1227–49.

Wahyuni, S., Prasetya, A., Kartini, I. (2017) Photocatalytic activity and antimicrobial properties of TiO_2-SiO_2-PVA composite. *Asian Journal of Chemistry,* **29**(2), 287-290.

White, T.J., Bruns, T., Lee, S., Taylor, J., (1990) "*PCR Protocols*", San Diego Academic Press, pp. 315–322.

Widyaningsih, W., Sofia, V., Yuliani, S., Rahmawati, Y., Nahda, R., Kemuning, D.H., Gustin, A. (2023) Wound healing activity of ethanol extract of green algae (*Ulva lactuca* L.) gel in mice. *Pakistan Journal of Pharmaceutical Science,* **36**(4), 1169-1176.

WU, S., Zhou, W. (2023) A review of oridonin, Antimicrobial activity of oridonin. *Food Science and Technology Campinas,* **43**,1-8.

Yahia, W.A., Elkhawaga, M.A., Mahfouz, A.Y., Attia, M.S. (2023) Achieving green synthesis of silver nanoparticles by *Aspergillus ustus* ON076464 forImproving immune response and vegetative growth of pepper plant towards wilt disease caused by *Fusarium oxysporum*. *Egyptian Journal of Chemistry,* **66**(7) 131-151.

Ziental, D., Czarczynska-Goslinska, B., Mlynarczyk, D.T., Glowacka-Sobotta, A., Stanisz, B., et al. (2020) Titanium dioxide nanoparticles: Prospects and applications in medicine. *Nanomaterials*, **10**, 387.

Zomorodian, K., Pourshahid, S., Sadatsharifi, A., Mehryar, P., Pakshir, K., et al. (2016) Biosynthesis and characterization of silver nanoparticles by *Aspergillus* species. *Biomedical Research International Journal*, Article ID 5435397, 6 pageshttp://dx.doi.org/10.1155/2016/5435397

التخليق الحيوى والتوصيف لجسيمات ثاني أكسيد التيتانيوم النانوية بواسطة الأسبرجلس نيجر DS22 وتطبيقاتها المحتملة في المجالات الطبية

داليا كمال عبد الحميد[1]، عنايات محمود دسوقى[1]، سوسن عبد الغنى عبداللطيف[2]، نيرمين نصرالدين عابد[1]، أميرة يحيى محفوظ[1]

[1]قسم النبات و الميكروبيولوجى- كليةالعلوم بنات جامعة الأزهر - مدينة نصر- القاهرة- مصر، [2]قسم تطوير الصناعات - معهد الهندسة الوراثية- مدينة الأبحاث العلمية والتطبيقات التكنولوجية- مدينة برج العرب الجديدة الأسكندرية -مصر.

حظيت المواد النانوية بإهتمام كبير في العقدين الأخيرين، وتم إدخالها في معظم مجالات الحياة، وخاصة المجال الطبي. ولذلك، يهدف البحث الحالي إلى التخليق الحيوي لجسيمات ثاني أكسيد التيتانيوم النانوية بواسطة *Aspergillus niger* DS22 (ON076463.1)وتقييم أنشطتها المضادة للبكتيريا والمضادة للإلتهابات والتئام الجروح. تم عزل خمس وأربعون عزلة فطرية من تسع عينات مختلفة من التربة المصرية وإختبارها لإنتاج جزيئات ثاني أكسيد التيتانيوم النانوية. تم تعريف العزلة الفطرية الواعدة بواسطة RNA الريبوسومي18 S باسم *Aspergillus niger* DS22 (ON076463.1). وتم تحسين العوامل التي تؤثر على إفراز المركبات النشطة بيولوجيًا المساعدة في التخليق الحيوي لجسيمات TiO_2 النانوية. أظهر التحليل اللوني للغاز - قياس الطيف الكتلي (GC – MS) وتحليل اللوني السائل عالي الأداء (HPLC) لمرشح*Aspergillus niger* DS22 (ON076463.1)، وجود مواد نشطة بيولوجيا. أظهرت النتائج أن جزيئات ثاني أكسيد التيتانيوم النانوية كانت بيضاوية إلى كروية الشكل، ويتراوح حجمها من 10.4 إلى 45.8 نانومتر بمتوسط حجم 26.619 ± 7.577 نانومتر. كان لجزيئات ثاني أكسيد التيتانيوم النانوية تأثير مضاد للبكتيريا ضد خمس سلالات بكتيرية ممرضة. كان الحد الأقصى للنشاط ضد المكورات العنقودية الذهبية المقاومة للميثيسيلين(MRSA (ATCC25923 (منطقة تثبيط 34 مم) وكان الحد الأدنى للنشاط ضد *Klebsiella pneumonia* (ATCC700603) (منطقة تثبيط 19.66 مم). أيضًا، أظهرت تثبيط لتحلل كريات الدم الحمراء البشرية بنسبة (97.7٪) عند تركيز 1 ملى جرام / مل مقارنة مع الإندوميتاسين القياسي (98.6%). علاوة على ذلك، كانت لها فعالية في شفاء جروح خلايا الجلد البشرية بعد 48 ساعة بنسبة (65.96%) مقارنة بالمادة القياسية (58.49%). أشارت هذه الدراسة أن جزيئات ثاني أكسيد التيتانيوم النانوية لها تأثيرات واعدة مضادة للبكتيريا، وشفاء الجروح، ومضادة للالتهابات، والتي قد تكون نهج مبشر للتطبيقات الصيدلانية.